

学位論文

**Identification of the *NSF* gene mutation that causes
abnormal Golgi morphology in *Arabidopsis thaliana***

(シロイヌナズナのゴルジ体形態異常を示す*NSF*遺伝子変異の同定)

平成29年 12月 博士 (理学) 申請

東京大学大学院理学系研究科

生物科学専攻

棚橋 沙由理

Abstract

The Golgi apparatus is a key station of glycosylation and membrane traffic. It consists of stacked cisternae in most eukaryotes. However, the mechanisms how the Golgi stacks are formed and maintained are still obscure. The model plant *Arabidopsis thaliana* provides a nice system to observe Golgi structures by light microscopy, because the Golgi in *A. thaliana* is in the form of mini-stacks that are distributed throughout the cytoplasm. To obtain a clue to understand the molecular basis of Golgi morphology, I took a forward-genetic approach to isolate *A. thaliana* mutants that show abnormal structures of the Golgi under a confocal microscope. In this thesis, I describe characterization of one of such mutants, named #46-3. The #46-3 mutant showed pleiotropic Golgi phenotypes. The Golgi size in #46-3 was in majority smaller than in the wild type, but varied from very small ones, sometimes without clear association of *cis* and *trans* cisternae, to abnormally large ones under a confocal microscope. At the ultrastructural level by electron microscopy, queer-shaped large Golgi stacks were occasionally observed. By positional mapping, genome sequencing, and complementation and allelism tests, I linked the mutant phenotype to the missense mutation D374N in the *NSF* gene, encoding the *N*-ethylmaleimide-sensitive factor (NSF), a key component of membrane fusion. This residue is near the ATP-binding site of NSF, which is very well conserved in eukaryotes, suggesting that the biochemical function of NSF is important for maintaining the normal morphology of the Golgi.

Table of Contents

ACKNOWLEDGMENTS	4
CHAPTER 1	7
GENERAL INTRODUCTION	8
CHAPTER 2	19
INTRODUCTION	20
RESULTS	27
DISCUSSION	33
CHAPTER 3	65
GENERAL DISCUSSION AND PERSPECTIVES	66

ACKNOWLEDGMENTS

First of all, I would like to express my sincere appreciation to my supervisor, Professor Akihiko Nakano, for giving me the opportunity to do my dissertation work in his laboratory, and for his valuable guidance and encouragement throughout this work. I would also like to express my gratitude to Assistant Professor Tomohiro Uemura for not only sharing experimental materials but also helpful advice.

I would like to express my appreciation to Dr. Takashi Ueda (National Institute for Basic Biology) for his valuable advice. I also thank Ms. Keiko Shoda (RIKEN) for sharing materials and encouragement. I would like to show my appreciation to Dr. Chieko Saito (The university of Tokyo) and Dr. Kiminori Toyooka (RIKEN) for valuable technical support of electron microscopy. I thank to Dr. Tetsuya Kurata (Nara Institute of Science and Technology) and Dr. Tomoaki Sakamoto (Nara Institute of Science and Technology) for analysis of next-generation sequencing. I would like to show my gratitude to Dr. Emi Ito (International Christian University), Dr. Junpei Takagi (Konan University) and Dr. Yoko Ito (RIKEN) for valuable technical advice and insightful discussion. I thank Dr. Choi Seung-won (International Christian University), and all the member of Live Cell Super-Resolution Imaging Research Team (RIKEN) for valuable discussion and encouragement. I also thank all the Lab members of Developmental Cell Biology, especially Mr. Keita Muro and Mr. Yutaro Shimizu for technical supports, lively discussion and sincere encouragement a lot.

Lasty, I would like to my deep gratitude to my parents, brother, husband and dear daughter for heartfelt supports throughout the years.

ABBREVIATIONS

Arf1, ADP-ribosylation factor 1

CCV, clathrin-coated vesicles

COPI, coat protein complex I

COPII, coat protein complex II

EMS, ethyl methanesulfonate

ER, endoplasmic reticulum

NSF, *N*-ethylmaleimide-sensitive factor

PM, plasma membrane

Sar1, secretion-associated and ras-superfamily-related 1

SNAP, soluble NSF attachment protein

SNARE, SNAP receptors

TGN, the *trans*-Golgi network

CHAPTER 1

GENERAL INTRODUCTION

All eukaryotic cells have various intracellular organelles, which have unique distinct roles for cell viability. Single membrane-bound organelles have a sophisticated system of protein transport called “membrane traffic” (Szul and Sztul, 2011) (Figure 1). Each organelle is compartmentalized which is defined by a specific component of proteins (Derby and Gleeson, 2007). In membrane traffic, diversified RAB (“rat brain”), small GTPase and SNARE (soluble *N*-ethylmaleimide-sensitive factor attachment protein receptor) molecules play crucial roles between vesicles and organelles. First, Sar/Arf family protein, also small GTPase facilitates vesicle budding from donor membrane, and Rab/Ypt family protein does vesicle tethering and fusion to target membrane (Saito and Ueda, 2009). Subsequently, SNAREs directly carry out membrane fusion (Ryu et al., 2016). Vesicle-associated SNARE (v-SNARE) interacts with target membrane-associated SNARE (t-SNARE). To date, a categorization based amino acid sequence within the characteristic “SNARE domain” has been established (Hong, 2005). According to it, v-SNAREs correspond to R-SNAREs and t-SNAREs correspond to Q-SNAREs. Furthermore, the Q-SNAREs are classified into three sub groups, Qa-, Qb-, and Qc-SNAREs, based on amino acid sequence similarity (Hong, 2005). The supercoil of SNARE helical bundle is formed on the lipid bilayer; it is greatly stable and requires both energy input (Fasshauer et al., 1998) and a specific apposition of called zero layer residues for their disassembly (Scales et al., 2001). After cargo release, disassembly of

SNARE complex is directly driven by ATP hydrolysis, which due to *N*-ethylmaleimide-sensitive factor (NSF) with association of soluble NSF attachment protein (SNAP) (Cipriano et al., 2013; Matveeva et al., 1997). Re-primed SNAREs take part in next round membrane fusion and these processes continuously occur in the living cells (Ryu et al., 2016).

The Golgi apparatus exists in all eukaryotic cells, which was first discovered as the "internal reticular apparatus", a novel intracellular organelle by Camillo Golgi (Golgi, 1898). He observed it in the Purkinje cells of the cerebellum by the silver impregnation for the staining of the nervous system. (Ito et al., 2014; Mazzarello et al., 2009). Because of insufficient microscopic techniques at that time, however the presence of the structure was under a debate for many years. Over half a century of controversy in the mid-1950s, the application of electron microscopy demonstrated its existence (Dalton, 1951; Dalton and Felix, 1954) and since then, it has been revealed that secretory cargoes pass across the Golgi apparatus (Dunphy and Rothman, 1985; Klumperman, 2011; Luini, 2011).

The Golgi apparatus plays crucial roles in cargo sorting and processing such as glycosylation and usually consists of flattened disk-shaped membrane sac termed cisternae, each of which has distinct processing enzymes (Klumperman, 2011) (Figure 2). These enzyme distributions show a conserved *cis*-to-*trans* polarity that reflects the order of oligosaccharide processing (Emr et al., 2009), thus early acting enzymes dominate in *cis*-cisternae, whereas late-acting enzymes are concentrated in

trans-cisternae (Nilsson et al., 2009). The *cis*-side cisternae receive newly synthesized proteins from the endoplasmic reticulum (ER), which travel across the stack to the *trans*-side cisternae. Then they are sorted in the *trans*-Golgi network (TGN) and eventually transported to their final destinations such as outside of the cell, the plasma membrane (PM) and lysosomes/vacuoles. Coat protein complex II (COPII)-coated vesicles carry newly synthesized proteins from the ER to the Golgi in anterograde way (Matsuoka et al., 2001; Sato and Nakano, 2007; Suda et al., 2018) and coat protein complex I (COPI)-coated vesicles retrieve proteins such as the H/KDEL receptor from the Golgi to the ER in retrograde way and also within the Golgi in a similar manner (Martinez-Menárguez et al., 2001; Nakano, 2015; Orci et al., 1997, 2000; Rabouille and Klumperman, 2005). Clathrin-coated vesicles (CCV) work in the TGN and post-Golgi compartments (Kang et al., 2011; Takei and Haucke, 2001). Vesicle formations of COPI- and COPII-coated are controlled by Arf1 (ADP-ribosylation factor) and Sar1 (secretion-associated and ras-superfamily-related) small GTPases, respectively (Glick and Nakano, 2009).

There has been a debate about how cargo proteins are transported in the Golgi (Glick, 2000; Glick and Malhotra, 1998; Pelham, 1998; Pelham and Rothman, 2000; Rabouille and Klumperman, 2005) (Figure 3). From mammalian-cell-based cell free assays, the vesicular transport model has been proposed, which assumes that the Golgi cisternae are stable static compartments and resident Golgi proteins are retained in the cisternae, while cargo proteins are conveyed by vesicles in the anterograde way (Rothman and

Wieland, 1996). Another model, called the cisternal maturation model derived cisternal progression model, considers that resident Golgi proteins move from later to earlier cisternae, thereby cisternae mature from *cis* to *trans*. Cargo can just stay in cisternae and eventually reach the *trans* side. This model was strongly supported by live imaging in the budding yeast *Saccharomyces cerevisiae* (Losev et al., 2006; Matsuura-Tokita et al., 2006), which clearly demonstrated that Golgi cisternae change their properties from *cis* to *trans* over time. In either of the two models, vesicles are believed to play critical roles in transport. General mechanisms of vesicular transport should apply to these intra-Golgi events. Namely, vesicles are formed by the budding machinery, which comprises COPI and the Arf GTPase, and are targeted to a particular cisterna by the fusion machinery, which involves tethers, Rab GTPases, NSF, SNAP and SNAREs. One reason why the cisternal maturation model is supported is because can explain the transport of large secretory cargo such as scale in algae (Becker et al., 1995) and procollagen in mammalian fibroblast (Bonfanti et al., 1998; Leblond and Inoue, 1989). Indeed, the cisternal maturation in yeast is strictly controlled by COPI, again supporting the main frame of the model (Ishii et al., 2016; Papanikou et al., 2015). It should also be noticed, however, that tubular extensions and interconnections can also play roles in intra-Golgi transport (Glick and Luini, 2011; Glick and Nakano, 2009) where COPI proteins bidirectionally regulate in both vesicular and tubular transport (Nakano, 2015; Park et al., 2015; Yang et al., 2011).

The Golgi consists of stacked cisternae in most eukaryotes. This principal structural

future of the Golgi is considered to reflect its function such as efficient transport and correct processing in order (Mollenhauer and Morré, 1991). There are marked variations among organisms in the morphological and organizational patterns of the Golgi (Figure 4).

In the budding yeast *S. cerevisiae*, the Golgi does not form stacks and individual cisternae as transient structures are dispersed in the cytoplasm (Losev et al., 2006; Matsuura-Tokita et al., 2006; Preuss et al., 1992). In *Pichia pastoris*, the other budding yeast strain, the Golgi shows the stacked structure and each Golgi is dispersed throughout the cytoplasm whereas the number of the Golgi is fewer than that in *S. cerevisiae* (Mogelsvang et al., 2003; Rambourg et al., 1995). In mammalian cells by contrast, the Golgi forms a giant and complex structure called “Golgi ribbon”, which is densely concentrated to the perinuclear centrosomal region (Ladinsky et al., 1999, 2002). In flowering plants such as *Arabidopsis* and tobacco, the Golgi is in the form of mini-stacks of cisternae, which are individually functional units, being distributed throughout the cytoplasm and moving along actin filaments (Ito et al., 2017; Staehelin and Kang, 2008). In some green algae such as *Scherffelia dubia*, the Golgi represents a large stack consisting of a numerous cisternae (Donohoe et al., 2007, 2013; McFadden and Melkonian, 1986; Staehelin and Kang, 2008). The Golgi apparatus in flowering plants is thus regarded as a nice model to study its morphology in detail by light microscopy (Faso et al., 2009; Hanton et al., 2005; Matheson et al., 2005). In spite of morphological and functional studies of the Golgi apparatus, the question what the significance of the peculiar stacked structure is given to it in most eukaryotic organism

is yet to be answered.

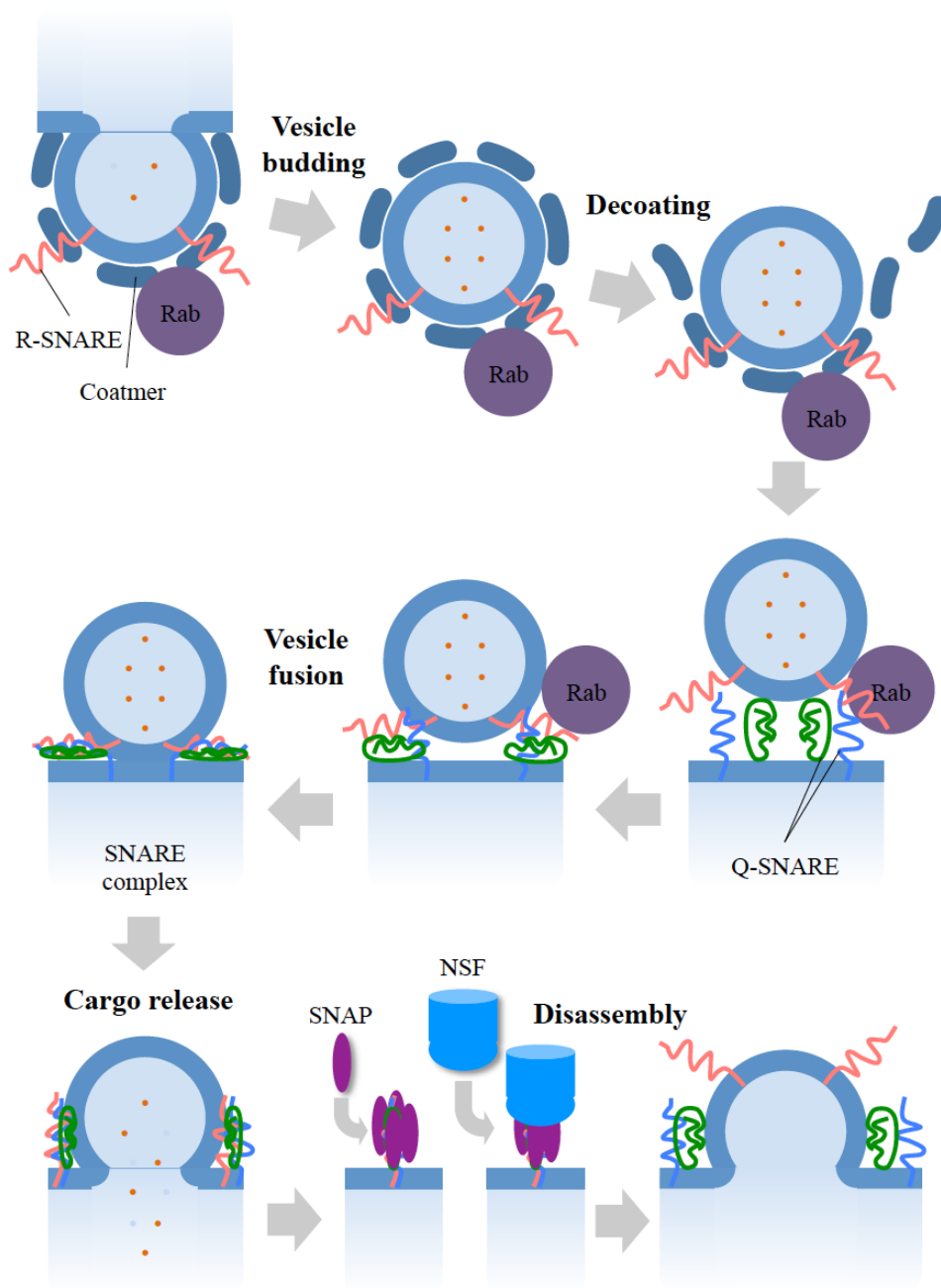


Figure 1. Illustration of membrane fusion in membrane traffic.

Vesicle budding occurs on donor membrane with facilitation by small GTPase such as Sar1/Arf1 and Rab. Coatmer is decoated during vesicle transport. Vesicle associates with acceptor membrane with facilitation by Rab. The SNARE complex consists of Q-SNAREs and R-SNARE, bridging two fusing membranes and cargoes are released. NSF disassembles the SNARE complex by ATP hydrolysis with co-factor, SNAPs (Ryu et al., 2016; Saito and Ueda, 2009).

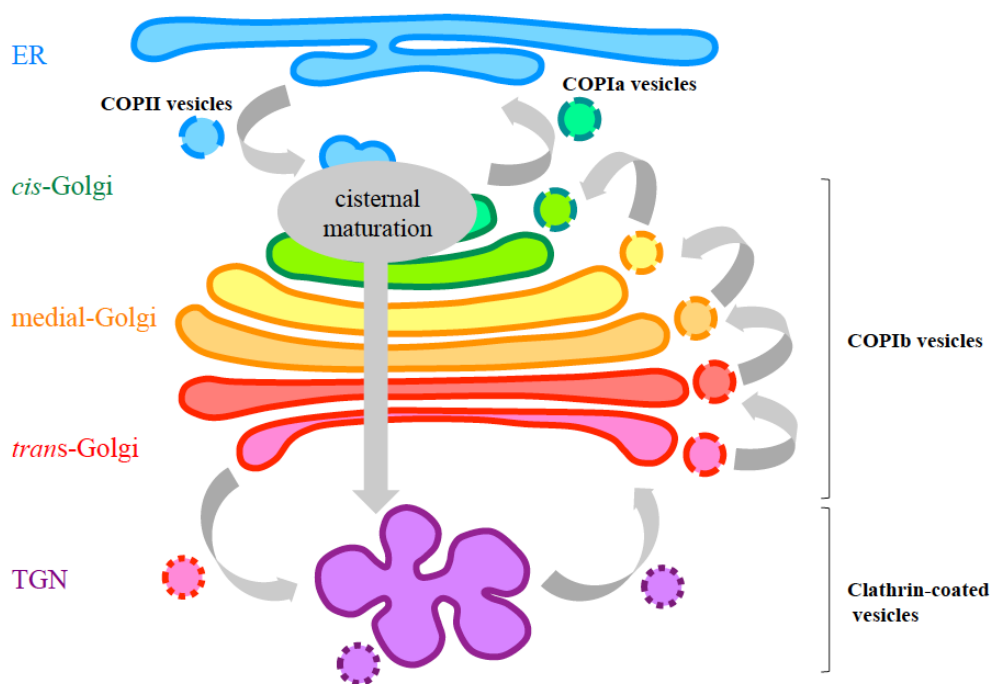


Figure 2. Structure of the Golgi and intra-Golgi trafficking.

COPII vesicles bud from the ER and fuse homotypically each other to form a *cis*-most cisterna and this cisterna grows full-size cisterna. ER-resident proteins are recycled from a *cis*-most cisterna to the ER via COPIa vesicles. A progression occurs from *cis* to medial and *trans* cisternae. Both medial and *trans* cisternae are involved in cargo glycosylation and material retrievals are carried out via COPIb vesicles when the nature of the cisternae gradually changes as they progress (Glick and Nakano, 2009; Ito et al., 2014; Nakano and Luini, 2010).

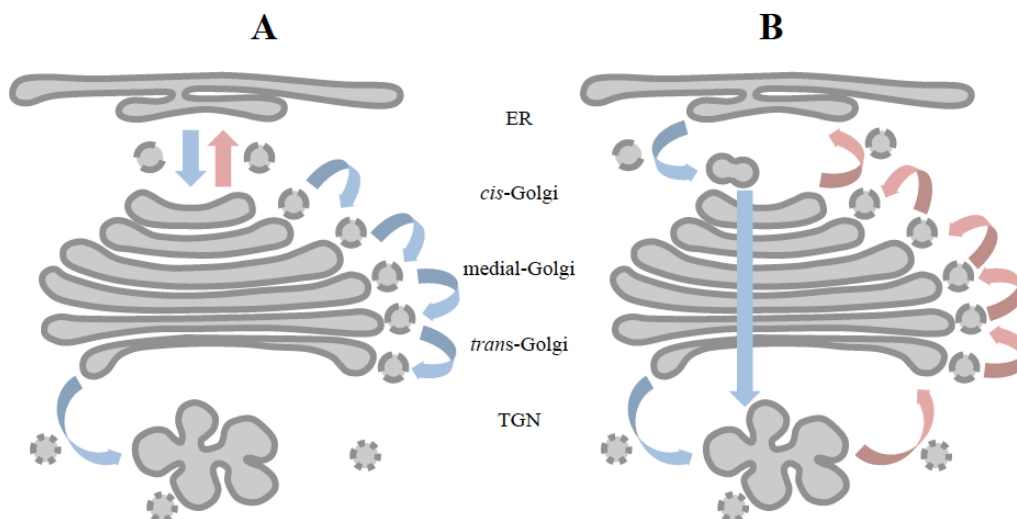


Figure 3. Two models for intra-Golgi trafficking.

(A) The vesicular transport (stable compartments) model. In this model, the Golgi stacks are stable static compartments, and resident Golgi proteins are retained in the cisternae while cargo are conveyed by vesicles in the anterograde way.

(B) The cisternal progression/maturation model. In this model, resident Golgi proteins move from older to younger cisternae, thereby new cisternae matures from *cis* to *trans*.

Blue arrows and pink arrows are indicated anterograde way and retrograde way, respectively (Glick and Nakano, 2009; Ito et al., 2014; Nakano and Luini, 2010).

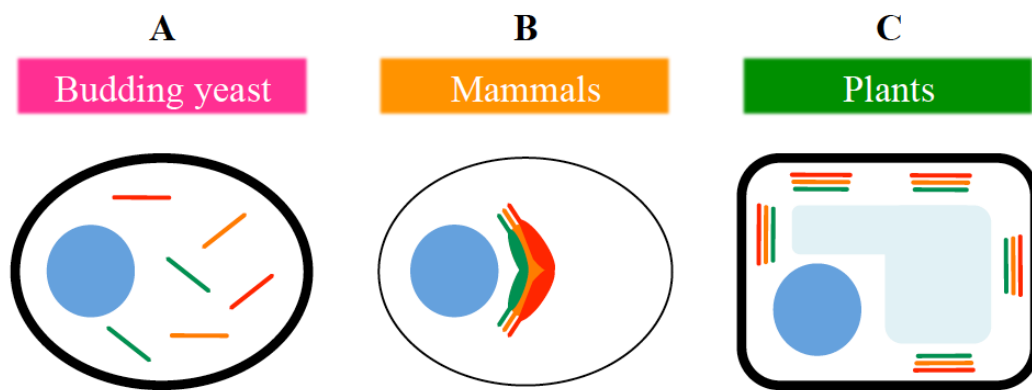


Figure 4. Comparison of Golgi organization among eukaryotic organisms.

- (A) In Budding yeast *Saccharomyces cerevisiae*. The Golgi does not show stacking and individual cisternae as transient structures are dispersed in the cytoplasm (Losev et al., 2006; Matsuura-Tokita et al., 2006; Preuss et al., 1992).
- (B) In mammalian cells. The Golgi forms a giant and complex ribbon-shaped structure, which is densely centralized to perinuclear centrosomal region in mammals (Ladinsky et al., 1999, 2002).
- (C) In plants. The Golgi is in the form of mini-stacks of cisternae, which are individually distinct and functional units, distributing throughout the cytoplasm and moving along actin filaments (Donohoe et al., 2007, 2013; Staehelin and Kang, 2008).

CHAPTER 2

INTRODUCTION

Molecular mechanisms of the membrane traffic have been investigated in plant cells, as following the studies from yeast and mammal (Nakano, 2004; Saito and Ueda, 2009; Südhof, T.C. 2013). Many studies have revealed that plants use similar machinery to mammals and fungi, while plant-specific molecules also participate in regulating their unique phenomena in plant life (Saito and Ueda, 2009; Ueda and Nakano, 2002). In endomembrane system of eukaryotic organisms, the secretory pathway comprises a numerous number of morphologically and functionally distinct organelles, which act together for extracellular environmental stimuli and maintenance of cell homeostasis.

In membrane traffic of eukaryotic cells, the Golgi apparatus is a key station of glycosylation and one of the most beautiful and elaborate organelle. The Golgi consists of cisternae, which usually are organized into polarized stacks and looks like a “pancake”. The number of cisternae per Golgi stack ranges from three to, sometimes hundreds cisternae depending the organisms and their cell types. The plant Golgi apparatus forms distinct individual mini-stacks and they are dispersed throughout the cytoplasm and move on actin filaments driven by myosin motors so-called the actomyosin system (Boevink et al., 1998; Hawes et al., 2008; Nebenführ et al., 1999). Each Golgi stack shows clear *cis-trans* polarity due to in order of oligosaccharides modified by a series of glycosylation enzymes that reside at characteristic locations

(Emr et al., 2009; Nilsson et al., 2009). The way of intra-Golgi trafficking, cisternal maturation model is more favored and supportive during cargo transport (Figure 3). Then, it was recently proposed that the Golgi underwent three stages. According to it, it is cisternal assembly, carbohydrate and carrier formation stage (Day et al., 2013; Papanikou and Glick, 2014). Initially, COPII-coated vesicles bud from the ER where taken place at specialized ER exit site (ERES) (Robinson et al., 2015; Stealin and Kang, 2008; Tang et al., 2005). How to transport proteins from the ER to the Golgi has been controversy whether new *cis* cisterna is born *de novo*, because in mammals ER-Golgi trafficking is carried out via ER-Golgi intermediate compartment (ERGIC) and travels along microtubules to the Golgi ribbon (Appenzeller-Herzog and Hauri, 2006.), but plant cells seem not to employ ERGIC (Day et al., 2013). Ito and her colleagues showed that Golgi regeneration was accomplished from *cis* to *trans* in order after fungal toxin Brefeldin A (BFA) washout in tobacco BY2 cells with super-resolution confocal live-imaging microscopy SCLIM (2012). Amazingly, she most recently demonstrated that in ER-Golgi trafficking cargo transport did via a COPII-independent scaffold named Golgi entry core compartment (GECCO) (Ito et al, 2018). Subsequently, COPII-coated vesicles fuse homotypically each other and assemble to form a *cis*-most cisterna while ER-resident proteins are recycled from a *cis*-most cisterna to the ER via COPIa-coated vesicles in plant cells (Day et al., 2013; Donohoe et al., 2013). Thus, COPII coat assembly is initiated by activating Sar1 GTPase with its guanine nucleotide exchange factor (GEF), Sec12 (Barlowe and Schekman, 1993; Nakano and Muramatsu, 1989). COPII coat complex including Sec23/24 and Sec13/31 are recruited in turns (Bi

et al., 2007; Matsuoka et al., 2001; Sato and Nakano, 2005). Sequentially, a *cis*-most cisterna grows full-size cisterna and a progression occurs from *cis* to medial and to *trans* cisternae. Both medial and *trans* cisternae are mainly involved in cargo glycosylation and material retrievals that are carried out via COPIb-coated vesicles when the nature of the cisternae gradually changes as they progress. COPI-coated vesicle formations are regulated by activating Arf1 GTPase with its GEF, a conserved Sec7 catalytic domain (Jackson and Casanova, 2000) such as GBF and BIG. COPI-coated vesicles are generated on the Golgi cisternal rims and the rims are occupied by numerous numbers of the vesicles (Donohoe et al., 2007; Pimpl et al., 2000; Ritzenthaler et al., 2002). Notably, it was showed that in plant cells ARF1 also localized to the Golgi cisternal rims (Ritzenthaler et al., 2002; Xu and Scheres, 2005). The characterization and identification of these coat proteins (COPII, COPIa and COPIb) so-called “coatmer” (Serafini et al., 1991; Waters et al., 1991) were achieved in according to their morphological features as size and electron density in electron topographic micrograph of rapidly frozen cells (Donohoe et al., 2007, 2013; Stealin and Kang, 2008). Then, it has also been revealed that basic common machineries involved in tubular connections are employed intra-Golgi trafficking among eukaryotic organism (Glick and Luini, 2011; Glick and Nakano, 2009, Nakano, 2015).

To further comprehend functional integrity of plant membrane traffic, combined microscopic technique with fluorescent protein variants has been demonstrated how plant homologues that are known their roles in non-plant cells and plant-specific

proteins that have unknown roles did work in the cells. By completion of a whole-genome sequencing of *Arabidopsis thaliana*, explosive genomic information allowed researchers to be available (Arabidopsis Genome Initiative, 2000). Moreover, recent next-generation sequencing techniques for mapping mutation have been remarkably developed (Austin et al., 2011; Schneeberger and Weigel, 2011; Uchida et al., 2011), reducing the time and labor for classical fine mapping. Combined with these tools, the development of forward genetic screens has led to identify various mutants of the secretory and the endocytic pathway (Sparkes and Brandizzi, 2012). The screens are based on identification of the structure labeled fluorescent marker such as green fluorescent protein (GFP), which exhibits morphological phenotype that is different from the wild type. Then it is widely known that ethyl methanesulfonate (EMS) mutagenesis generates point mutations in the genomic DNA and it is therefore expected to isolate missense mutants. The EMS mutant is assumed to show knockdown of gene function whereas the T-DNA (transfer DNA) mutant is considered to completely knockdown of that and may be lethal. Several examples of identification and characterization mutants whose responsible genes work at organelles located in the secretory pathway by visual screens are mentioned below.

First, screens of ER morphology defects using the ER luminal marker GFP-h identified two *ermo* (*endoplasmic reticulum morphology*) mutants displaying ER-derived abnormal spherical bodies (Nakano et al., 2009). Large globular aggregates were observed in *g92/ermo2* cells and the mutation was mapped to a missense mutation in

AtSEC24A (Faso et al., 2009; Nakano et al., 2009), which was one of the Arabidopsis isoforms encoding the COPII protein SEC24. The complete loss of AtSEC24A is lethal, but AtSEC24A perhaps shares their functions with the two other AtSEC24 isoforms. As another example, the small vacuolar protein labeled ST-GFP, a *trans*-Golgi marker (sialyl transferase from rat) (Boevink et al., 1998), mislocalized to and retained into the ER in *gold36* (*Golgi defective 36*) mutant (Marti et al., 2010). Thereafter, it was demonstrated that development of ER body (Matsushima et al., 2001) were observed in a certain type of cells of *ermo/mvp1/gold36* mutant, and suggested that ERMO3/MVP1/GOLD36 then was required for maintenance of ER morphology and integrity, and was pivotal for ER body-related defense systems (Nakano et al., 2012). One more example shows a mutant exhibiting aberrant ER morphology. Screen based on the distribution of sec-GFP, sporamin signal peptide to GFP showed that identification of the ROOT HAIR DEFECTIVE 3 allele (*rhd3-1*), which an ER-anchored GTPase required for maintenance of ER morphology and supposed that RHD3 was important for ER-Golgi trafficking (Orso et al., 2009; Zheng et al., 2004). Arabidopsis has three RHD3 isoforms that are homologous to the yeast Sey1p and to the mammalian atlastin GTPases involved in formation of ER tubules (Chen et al., 2011; Zhang, and Hu, 2013). Accordingly, it was suggested that molecular mechanisms regulating ER tubules might not be entirely conserved among eukaryotes because Arabidopsis RHD3 and Sey1p were not interchangeable each other (Chen et al., 2011).

Moreover, I mentioned one prominent discovery that mutant screens using sec-GFP, it is the identification and characterization of a *gnome-like 1* (GNL1) (The and

Moore, 2007). GNL1 is the closest homolog of Arabidopsis GNOM, which was first identified as a GBF-ARF GEF in plants. GNOM was found to act in recycling of auxin efflux carrier PIN1 from endosomes to the PM (Geldner et al., 2003). Thereafter, it was demonstrated that GNL1 localized at the Golgi stack where regulated coatmer recruitment and, was involved in ER-Golgi trafficking (Naramoto et al., 2014; Richter et al., 2007, 2010). The study clarified that GNL1 was BFA resistant unlike GNOM was BFA sensitive and that they played roles in selective endocytic pathway and in maintenance of Golgi morphology. In *gnl1* mutant, the Golgi stack was approximately 50% larger than the wild type (The and Moore, 2007). Additionally, it was revealed that *ermol* was *gnl1* mutant allele and that GNL1/ERMO1 was responsible for organizing and maintaining ER structure (Nakano et al., 2009). These finding suggested that plant ARF GEF might not only act on various secretory unlike mammal but also form and maintain the morphology of organelles.

Meanwhile, the screens using PIN1pro:PIN1-GFP, PIN1, an auxin efflux carrier, which localized to the PM at the basal side led to identify proteins affected trafficking (*pat*) mutants that showed strong partial accumulation of PIN1-GFP to aberrant vacuolar structures (Zwiewka et al., 2011). *pat* mutant phenotypes were caused by members of AP-3 adaptin complex, which were known as key regulators of cargo sorting into vesicles (Dell'Angelica, 2009). Thereby, it was manifested that AP-3 complex was present not only in yeast and mammal but also in plants. Furthermore, the AP-3 β adaptin could interact with clathrin, which was known to work in post-Golgi trafficking.

It was suggested that AP-3 complex might be given plant-specific roles for regulating biogenesis and the function of vacuoles (Feraru et al., 2010).

Finally, screens for Golgi defects was only reported that isolated several mutant candidates showing the abnormal distribution of the Golgi marker, ST-GFP (Boulaflous et al, 2008). However, there has been no evidence to identify a mutant whose responsible gene required for formation and maintenance of Golgi morphology in *A. thaliana*. To understand more about the elements in the mechanism how the Golgi stacks are formed and maintained, I decided to employ a forward-genetic approach combined with confocal microscopy-based visualization to isolate mutants from *Arabidopsis thaliana* that show abnormal morphology of the Golgi. Among 30 mutant candidates I isolated. In this thesis, I describe the identification and characterization of a recessive EMS mutant. I named the mutant #46-3, which shows aberrant structures in the stack under a confocal microscopy and an electron microscopy. The mutation responsible for the phenotype was point mutation that was experimented by a combination of positional mapping, genome sequencing, and complementation tests. Therefore, I concluded that a D-to-N missense mutation in the *NSF* gene, encoding a key factor in membrane fusion, is the cause of the phenotype.

RESULTS

Visualization of the Golgi in *Arabidopsis thaliana*

To isolate mutants that show abnormalities in the morphology of the Golgi apparatus, I decided to use the *A. thaliana* line that expresses ERD2-GFP driven by 35S promoter, a well-established *cis*-Golgi marker (Bar-Peled et al., 1995; Boevink et al, 1998; Takeuchi et al., 2000, 2002). The fluorescence of ERD2-GFP shows disk-like structures, which are dispersed through the cytoplasm. The parent line A21, expressing ERD2-GFP, was treated with ethyl methanesulfonate to induce mutations. After due processes, M2 lines were established and subjected to visual screen under a confocal microscope, Olympus IX81 equipped with a spinning-disk confocal unit CSU10. As the morphology of the Golgi appeared to vary in different tissues, I selected the third-leaf-petioles of 16-day-old seedlings, which reproducibly show large and bright Golgi structures (Figure 5).

Isolation of a mutant with abnormality in the Golgi morphology

By manual examination of approximately 10,000 M2 lines, I selected 30 mutant candidates that showed altered shapes of the Golgi. The morphological phenotypes were of a wide variety; large, small, with tubules, large and bent, large aggregates, and so on (Figure 6). They were further subjected to crossing with the parent to determine dominant or recessive natures. The mutant line named #46-3, which is the subject of

this thesis, displayed abnormalities in the size and shape of the Golgi and this phenotype turned out recessive to the wild type. Otherwise, the #46-3 mutant did not show any discernible macroscopic phenotypes. The mutant plants grew normally and were fertile (Figure 7).

Microscopic Golgi phenotype in #46-3 mutant

The abnormality of the Golgi morphology in #46-3 was the peculiarity of size and shape as shown in Figure. 8A. While the ERD-GFP fluorescence in the wild type showed mostly disk-like shapes in similar sizes, in the #46-3 mutant the shape looked irregular and the size varied from smaller to larger as compared to the wild type (Figure 8A and B). To quantify the Golgi size, I measured the areas of fluorescent signals in 10 epidermal cells of petioles (expressed as pixels). The distribution of the Golgi size in the wild type and in #46-3 is shown as histograms in Figure. 9. It clearly shows that the Golgi size of #46-3 is in majority smaller than the wild type. It should be noted that abnormally large Golgi was also occasionally seen in the #46-3 mutant (Figure 8C).

Localization analysis of *cis*- and *trans*-Golgi in the #46-3 mutant

To further investigate the anomalies of the Golgi morphology, the arrangement of *cis* and *trans* cisternae in Golgi stacks was examined in the wild-type and #46-3 plants stably expressing ST-mRFP, a *trans*-Golgi marker (Boevink et al., 1998; Boulaflous et al, 2008; Ito et al., 2012; 2017), in addition to ERD2-GFP (Figure 10). As shown in Figure 11, fluorescence signals of ERD2-GFP and ST-mRFP were mostly adjacent to

each other. Sometimes the distance between the peaks of GFP and mRFP signals was markedly larger in the #46-3 mutant. GFP signals without associating mRFP signal were also occasionally observed in the #46-3 mutant (Figure 12). Moreover, I compared the size of the *cis*-Golgi with that of *trans*-Golgi. Smaller *cis*-Golgi tended to associate with smaller *trans*-Golgi or none (Figure 13).

Electron microscopic analysis of the Golgi structure in the #46-3 mutant

I next analyzed the Golgi morphology in the #46-3 mutant by transmission electron microscopy. The Golgi stacks in the wild-type *Arabidopsis* usually consist of around 5 cisternae as shown in Figure 14A. Abnormally small Golgi structures, which were often seen in fluorescence, were not easy to identify in the leaf epidermal cells of #46-3, perhaps because they did not show typical stacks. Figure 14B shows one example of electron micrograph showing two Golgi-like structures harboring 2-3 cisternae. I sometimes observed abnormal Golgi stacks consisting of increased numbers of cisternae in the #46-3 mutant. In the example shown in Figure 14C, as many as 9 cisternae can be counted in what appeared to be a single Golgi stack. In another example (Figure 14D), a Golgi stack bore an unusually large *trans*-most cisterna. To quantify the cisternal number per Golgi stack, I counted that in the epidermal cells of petioles. The distribution of the cisternal number in the wild type and #46-3 is shown as histograms in Figure 15. The cisternal numbers did not appear significantly different in the Golgi stacks between the wild type and the #46-3 mutant, the latter showing a broader distribution. As mentioned above, abnormal Golgi that did not show typical stacks

might be overseen in electron micrographs. Combined with the fluorescence observation, I concluded that the #46-3 mutant had a pleiotropic defect in normal arrangement of Golgi stacks in both size and shape.

Rough map

To identify the mutation in the genome that caused the phenotype of #46-3, I proceeded to identify the mutation locus. I crossed the #46-3 plants with the wild-type plants (Col-0) expressing ERD2-GFP to determine the inheritance pattern. Segregation of the F2 population from the third backcross indicated that the #46-3 mutation was recessive to the wild type (Figure 16). To generate a mapping population, I crossed #46-3 with a different ecotype Landsberg *erecta*. The genomic DNA of F2 plants exhibiting the abnormal phenotype was roughly mapped with markers of simple sequence length polymorphisms (SSLPs) and cleaved amplified polymorphic sequence (CAPSs) (Konieczny and Ausubel, 1993; Bell and Ecker, 1994) (Figure 17).

Linkage analysis by next-generation sequencer

Then, the candidate region containing the mutation was analyzed by the linkage analysis using a next-generation DNA sequencer. The results of these analyses nailed down the causal mutation on the upper arm of the chromosome 4 at 1-5.5 Mbp interval (Figure 18). Among nucleotide differences within this region, only 3 were predicted to be non-silent in open-reading frames (Figure 19). They were in the loci At4g02410, At4g02750, and At4g04910, which were annotated to encode L-type lectin-like protein

kinase 1 (AtLPK1), tetratricopeptide repeat (TPR)-like superfamily protein, and *N*-ethylmaleimide-sensitive factor (NSF), respectively (Figure 20). Among these three, At4g04910 was of particular interest to me, because NSF is well known as a key protein required for membrane fusion.

Alignment of NSF amino acid sequence among eukaryotic organisms

The At4g04910 locus of #46-3 had a G-to-A point mutation at the nucleotide number 2492290, which led to a GAT to AAT codon change resulting in the amino acid change from aspartic acid to asparagine at the residue position 374 (D374N). *A. thaliana* has only one ortholog of NSF in the genome. Comparison of NSF sequences indicates that this aspartate residue is very well conserved in eukaryotes (Figure. 21).

Complementation test

To examine whether the D374 mutation in NSF was indeed responsible for the observed phenotype, I performed a complementation test. I cloned the genomic DNA fragment from the wild-type plants containing the whole At4g04910 locus including the promoter and the open-reading frame and introduced into the #46-3 mutant. I analyzed the Golgi morphology in leaf petioles of two independent T2 seedlings under a confocal microscope. As shown in Figure 22 and 24, the #46-3 phenotype in the Golgi shape and the Golgi size distribution was almost fully complemented. These plants genome extracted were genotyped using a primer set of the sequence both vector pHGW and *NSF* gene (Figure 23). DNA fragments containing At4g02410 or At4g02750 did not

complement the defect (Figure 25).

Allelism test

I also conducted an allelism test. I obtained from the ABRC stock center three *A. thaliana* lines containing T-DNA insertions at the *NSF* gene locus in the Col-0 background. I confirmed that T-DNA was inserted in the 5' UTR both in SALK_091598/SALK_138721 (at nucleotide 2495839) and in SAIL_1155_C06 (at nucleotide 2495824) and in the third exon in SAIL_620_E12 (at nucleotide 2495008) of the *NSF* gene (Figure 26). I could make a homozygous line of SALK_091598/SALK_138721 but not for SAIL_1155_C06 and SAIL_620_E12, probably because the complete knockout of NSF is lethal. Then, I crossed #46-3 with SAIL_1155_C06 to establish a heterozygous line and examined its Golgi morphology. As shown in Figure 27 and 28, the Golgi phenotype seen by ERD2-GFP signals in the transformed #46-3/SAIL_1155_C06 plant phenocopied that of the #46-3 mutant under a confocal microscope.

Taken together, I concluded that the D374 missense mutation in NSF caused the Golgi morphology phenotype of #46-3.

DISCUSSION

Morphology of organelles is considered to reflect their functions. Stacking of cisternae in the Golgi apparatus is one of the most striking structural features, which has been attracting many cell biologists, and is believed very important for efficient processing and sorting of cargo molecules. However, the fact that the budding yeast *S. cerevisiae* does not have a stacked structure of the Golgi yet managing efficient cargo processing leaves the significance of stacking elusive. From a mechanistic point of view, how these stacked structures are formed and maintained is also intriguing. The roles of Golgi matrix proteins have been argued for animal cells, but most of these molecules are not conserved in plants, whose Golgi nevertheless shows beautiful stacked structures. We have recently revealed by super-resolution confocal live imaging microscopy (SCLIM) (Kurokawa et al., 2013) that Golgi stacks in tobacco cells are formed in the order from *cis*- to *trans*-cisternae and that the presence of scaffold at *cis*-most side, which we named Golgi entry core compartment (GECCO), plays a role of receiving cargo from the ER (Ito et al., 2012, 2018). Furthermore, computational simulation has implicated self-organizing properties of Golgi cisternae during reassembly processes (Tachikawa and Mochizuki, 2017).

To obtain further insights into the molecular basis for Golgi morphogenesis in plant cells, I have sought for mutations that affect Golgi morphology in Arabidopsis by a forward-genetic approach. In this study, I have demonstrated that the mutant #46-3

has a D374N missense mutation in NSF, which is responsible for the morphological defect of the Golgi.

NSF is a key player in membrane fusion events

NSF, *N*-ethylmaleimide-sensitive factor, was first identified as a key protein functioning in intra-Golgi trafficking. Inactivation of the Golgi membrane by *N*-ethylmaleimide in a cell-free reconstitution system caused perturbation of intra-Golgi transport (Glick and Rothman, 1987). This assay allowed purification of NSF (Block et al., 1988; Malhotra et al., 1988). As interacting molecules with NSF, SNAP was isolated (Weidman et al., 1989), and as the membrane receptors for SNAP, SNARE proteins were discovered (Söllner et al., 1993). All these components are now known to constitute the pivotal machinery for membrane fusion.

NSF is a member of the ATPases associated with diverse cellular activities plus (AAA+) family, which are present in all kingdoms of eukaryotes (Erzberger and Berger, 2006; Iyer et al., 2004). The most important role of ATP hydrolysis by NSF is to disassemble the SNARE complex after membrane fusion (Owen and Schiavo, 1999). NSF is now known to be essential for numerous membrane fusion events (Südhof, 2013; Sutton et al., 1998; Weber et al., 1998).

As such, the NSF function is essential for many cellular activities and thus must be essential for life. Indeed, the *S. cerevisiae* *SEC18* gene that encodes NSF is essential for growth. Our results that *A. thaliana* lines that were homozygously null for NSF were never obtained from two T-DNA insertion lines (in this study), probably

indicate that the complete loss of NSF is lethal.

The missense mutation of NSF that we identified as the cause of the abnormal Golgi morphology was D to N substitution at the amino acid residue #374. A D-to-N mutation is often regarded as subtle because the structural change in the side chain is small. It is probably why this mutant was obtained without an appreciable growth phenotype. Microscopically, the phenotype of this mutant is pleiotropic. At the fluorescence confocal microscope level, the Golgi size was in majority smaller than the wild type, but varies from very small ones, sometimes without clear association between *cis* and *trans* cisternae, to abnormally large ones, which were rather rare. At the ultrastructural level by transmission electron microscopy, abnormally small Golgi structures were hard to find, perhaps because they did not look like typical Golgi, but queer-shaped large Golgi stacks were occasionally observed.

Asp374 in the NSF-D1 domain is highly conserved among eukaryotes

In the process of membrane fusion, several reactions proceed in a sequential manner. The leading player is the SNARE proteins; R-SNARE on the vesicle membrane and the Qa-, Qb- and Qc-SNAREs on the target membrane, form 4-helix bundles to execute physical fusion of two lipid bilayers. After fusion, the SNARE bundles have to be disassembled for the next round of fusion reactions. NSF and SNAP play roles in this SNARE disassembly. Hydrolysis of ATP by NSF is essential for the disassembly reaction.

The molecular structure of NSF has been analyzed by X-ray crystallography

(Lenzen et al., 1998; May et al., 1999). NSF consists of an amino-terminal region that interacts with other components of the vesicle trafficking machinery, followed by the two homologous ATP-binding cassettes, designated D1 and D2, which possess essential ATPase and hexamerization activities, respectively. The D374 residue of Arabidopsis NSF lies in the D1 domain near the ATP-binding site, around which the amino acid sequence is very well conserved among eukaryotes (Figure 21). Thus the D374N mutation of Arabidopsis NSF may well affect its ATP-binding or hydrolysis activities of NSF, which should be examined in detail on purified proteins in the future.

Membrane fusion and the Golgi morphology

Now the question is how the lesion of NSF can affect the Golgi structure. Is it the membrane fusion events that are directly involved in cisternal arrangements? Regardless the model of cargo transport within the Golgi, it is obvious that the membranes in the Golgi have to be in a very dynamic equilibrium. Vesicle budding and membrane tubulation together with membrane fusion events must be always going on to maintain the steady-state morphology of the Golgi. Finding of a missense mutation in NSF, the essential factor of fusion, will provide a clue to further understanding of how the beautiful structure of the Golgi is formed and maintained.

In sum of this study, I proposed a model the Golgi phenotypic changes in the #46-3 mutant (Figure 29). It is considered that disassembly of SNARE complex by NSF is slower due to missense mutation D374N. According to it, the equilibrium of intra-Golgi trafficking is little broken; Small Golgi observed under confocal microscopy

and decreasing the cisternal numbers per Golgi stack showed under electron microscopy in the #46-3 mutant is caused by delay of COPII vesicle disassembly on *cis*-most cisternae (Figure 29B). Putative Golgi stack therefore loses *cis*-to-medial maturing, resulting in small and bearing a few cisternae. In contrast, large Golgi observed under confocal microscopy, and increasing the cisternal numbers and the *trans*-most cisternal sizes per Golgi stack under electron microscopy is caused by delay of COPIb vesicle disassembly on medial/*trans* cisternae (Figure 29C). It was demonstrated that COPI protein was critically needed for Golgi cisternal maturation and dynamics (Ishii et al., 2016; Papanikou et al., 2015). Because each medial and/or *trans* cisternal maturing is probably prolonged, thereby visualized Golgi cisternae are large and/or more layered.

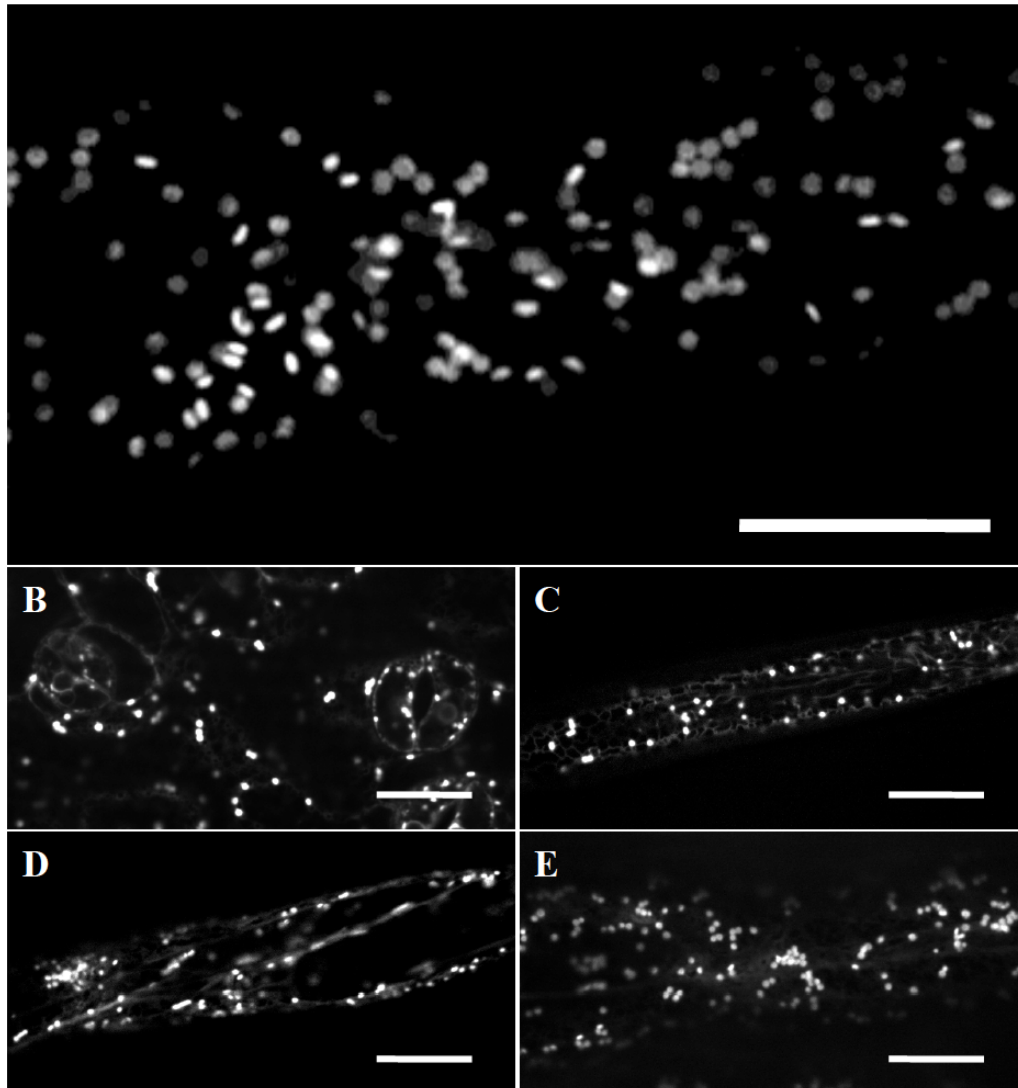


Figure 5. Visualization of the Golgi stacks in Arabidopsis living cells.

Confocal optical sections of the epidermal cells from the parent line A21 plants. The Golgi stack is disk-shaped structure and they are dispersed throughout the cytoplasm.

- (A) Epidermal of third-leaf-petioles at 16 DAG.
- (B) Trichome in the third-leaf at 16 DAG.
- (C) Epidermal cell in the leaf-blade at 16 DAG.
- (D) Epidermal cell in the cauline-leaf at 25 DAG.
- (E) Main root at 16 DAG.

Scale bar, 10 μm .

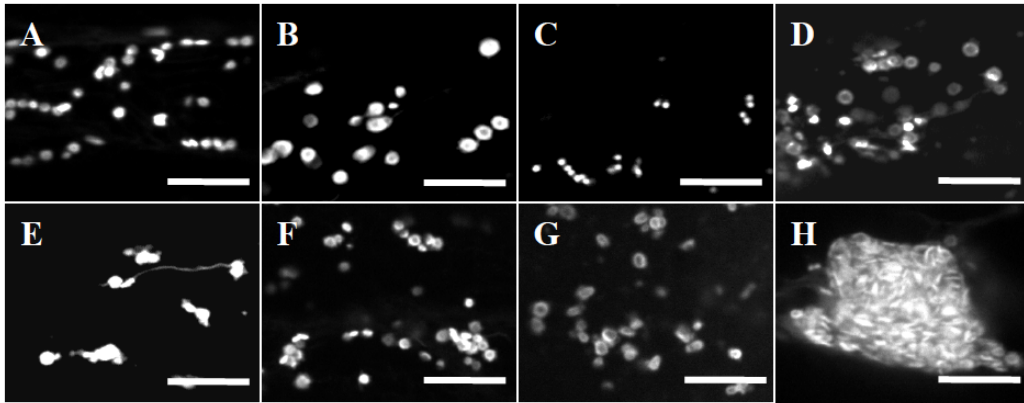


Figure 6. Mutant candidates show abnormal Golgi morphology.

Confocal optical sections of leaf epidermal cells of third-leaf-petioles from the M2 line cells.

- (A) The parent line A21 as wild type.
- (B) #14-6 shows the large Golgi.
- (C) #25-6 shows the small Golgi.
- (D) #38-5 shows the Golgi with different fluorescence.
- (E) #45-11 shows the Golgi with tubules.
- (F) #46-3 shows abnormalities in the size and shape of the Golgi.
- (G) #62-5 shows the large and bent Golgi.
- (H) #64-11 shows large aggregates of the Golgi.

Scale bars, 5 μ m.

Wild type

#46-3



Figure 8. The #46-3 mutant grow normally.

The #46-3 mutant exhibited no visible abnormal phenotype. Plants are 35 DAG.

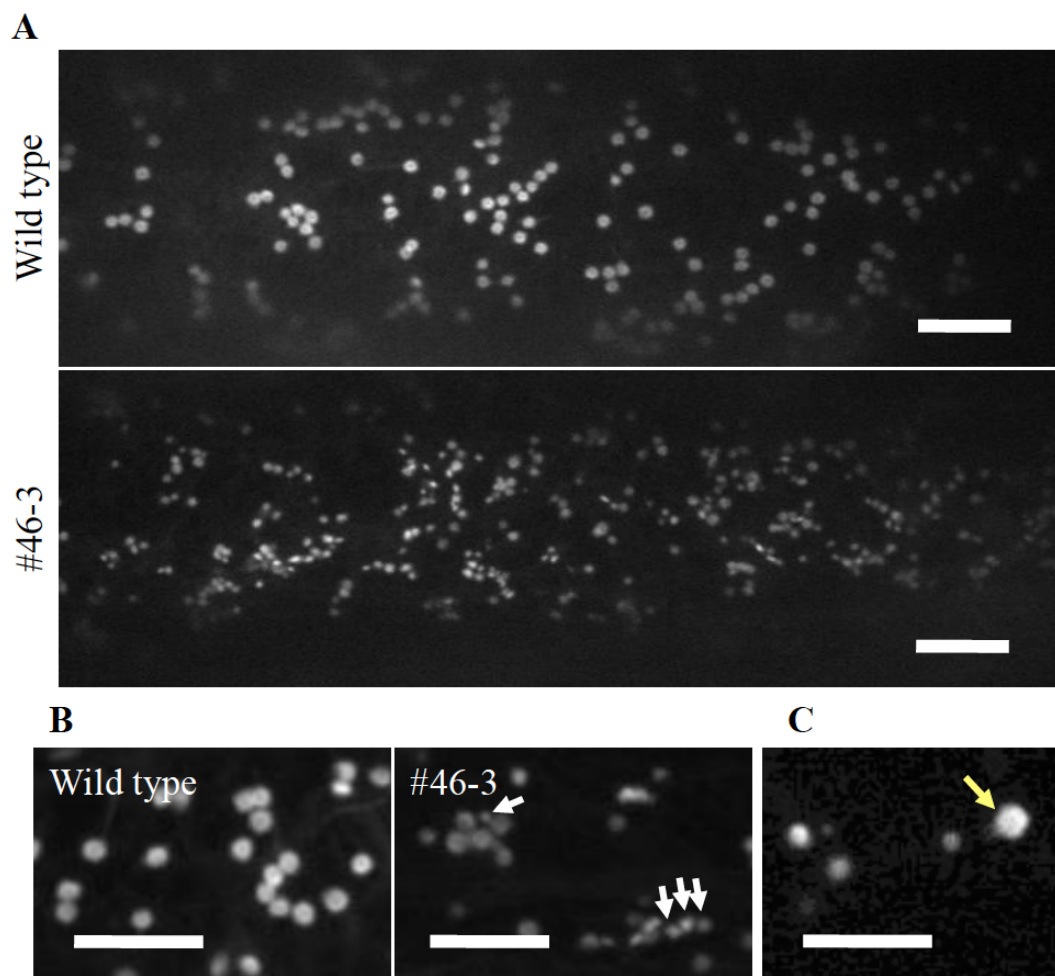


Figure 8. #46-3 shows an abnormal Golgi morphology.

- (A) Confocal optical sections of leaf epidermal cells of third-leaf-petioles from the wild-type and the #46-3 mutant *A. thaliana* cells. Scale bar, 5 μ m.
- (B) Close-up images of the wild-type and #46-3 mutant cells. White arrows indicate small Golgi structures in the #46-3 mutant. Scale bar, 5 μ m.
- (C) Abnormally large Golgi in the #46-3 mutant. Yellow arrow indicates large Golgi structures in the #46-3 mutant. Scale bar, 5 μ m.

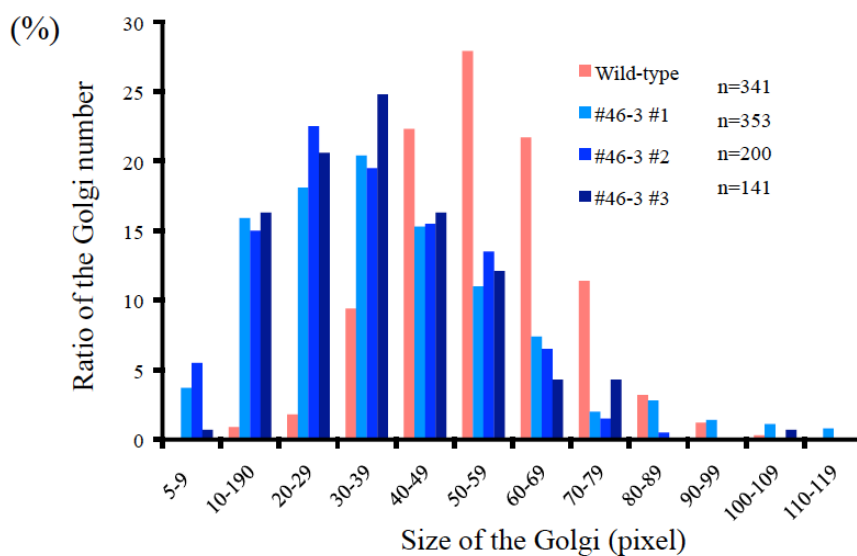


Figure 9. Comparison of the Golgi size between the wild type and independent three lines of the #46-3 mutant.

The Golgi sizes in 10 petiole cells were measured with ImageJ software and expressed as pixels.

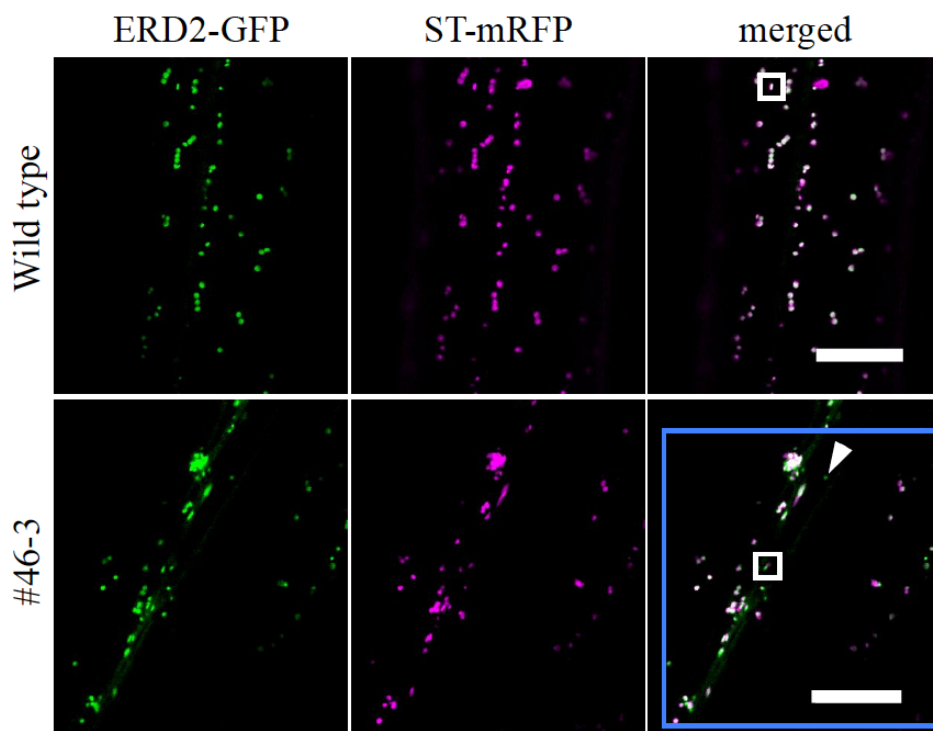


Figure 10. Localization analysis of the *cis*-Golgi marker ERD2-GFP and the *trans*-Golgi marker ST-mRFP.

Two confocal slices of epidermal cells of third-leaf-petioles of the wild type and the #46-3 mutant. Scale bars, 10 μ m.

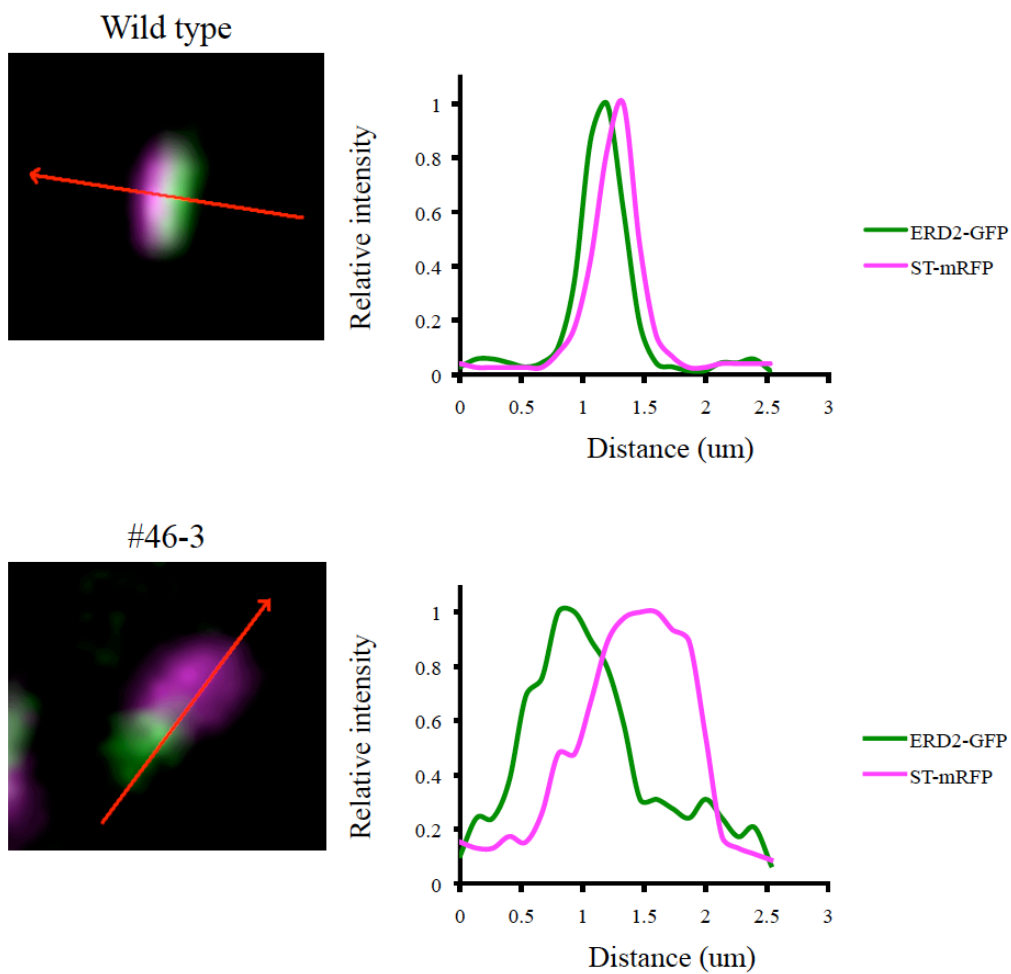


Figure 11. The fluorescence profile across the *cis-to-trans* Golgi stack.

The fluorescence profiles along the red arrows across the Golgi stacks indicated by white boxes in Figure 10. The intensity is shown relative to the maximum intensity in each signal of fluorescence, which is represented as 1.



Figure 12. *Cis*-Golgi without *trans*-Golgi.

A magnified view of the Golgi stack indicated by the arrowhead in Figure 10. Note the lack of the ST-mRFP signal.

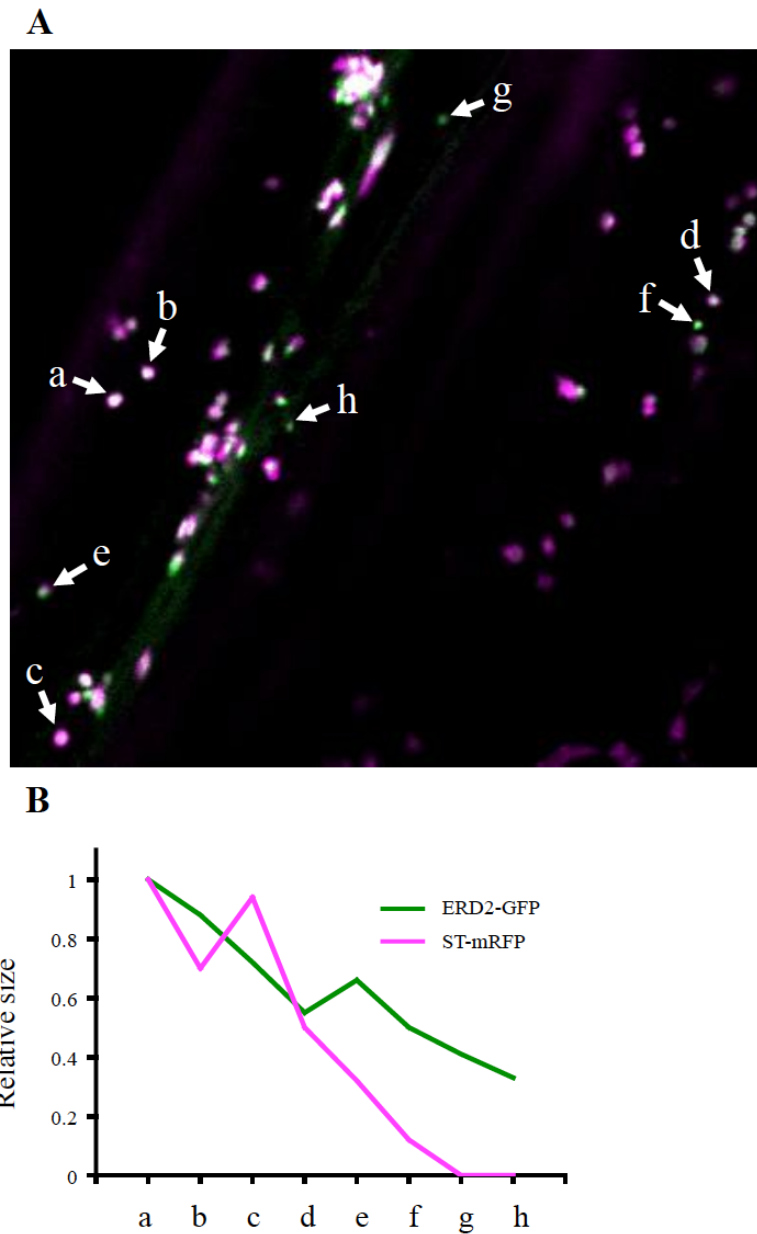


Figure 13. Comparison of the size of *cis*-Golgi and *trans*-Golgi between dependent 10 #46-3 mutant lines.

Confocal optical sections indicated by blue box in Figure 10. The size is shown relative to the maximum size in each signal of fluorescence, which is represented as 1. Smaller *cis*-Golgi tends to associate with smaller *trans*-Golgi or none.

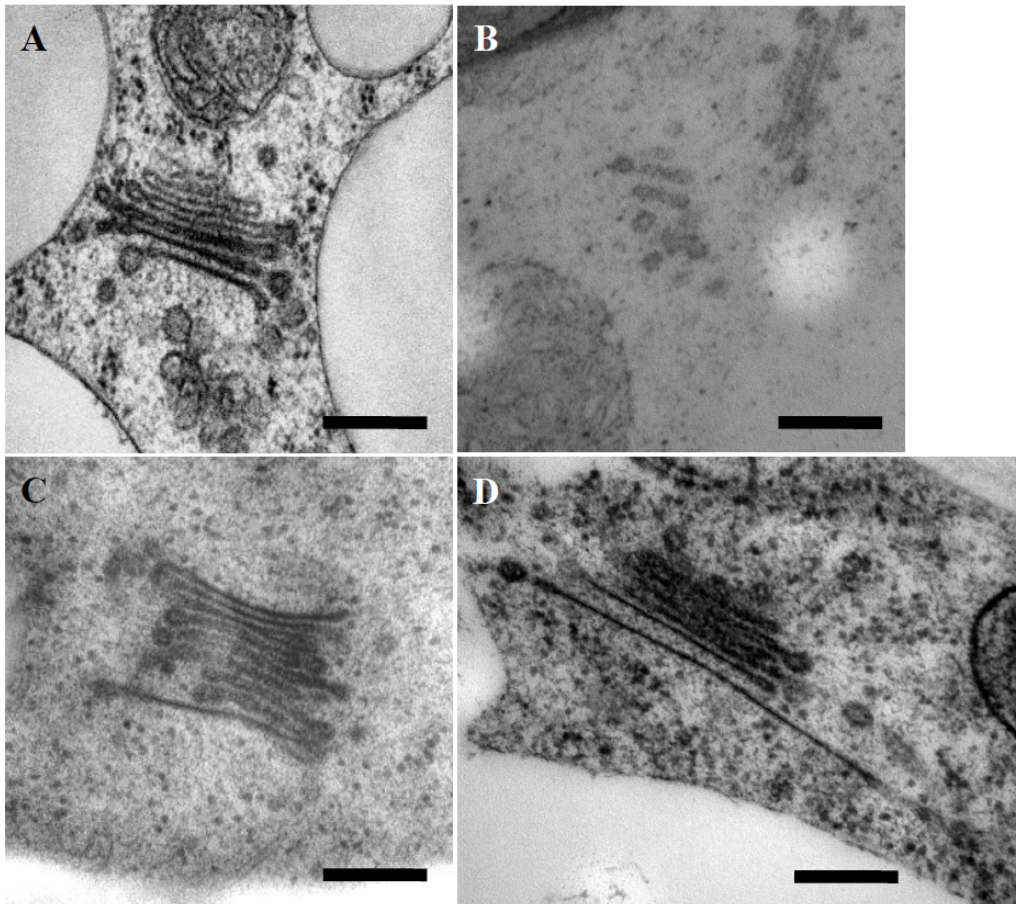


Figure 14. Ultrastructure of the abnormal Golgi morphology.

(A) An electron micrograph of the Golgi in the wild type. The cisternal number is 5 in this example.

(B-D) Electron micrographs of the Golgi in the #46-3 mutant. In (B), the structures did not look like typical Golgi stacks but appeared to have smaller number (2-3) of cisternae. In contrast, the cisternal number of the Golgi is increased in (C) and the Golgi stack bears an extremely large *trans*-most Golgi cisterna in (D). Scale bar, 200 nm.

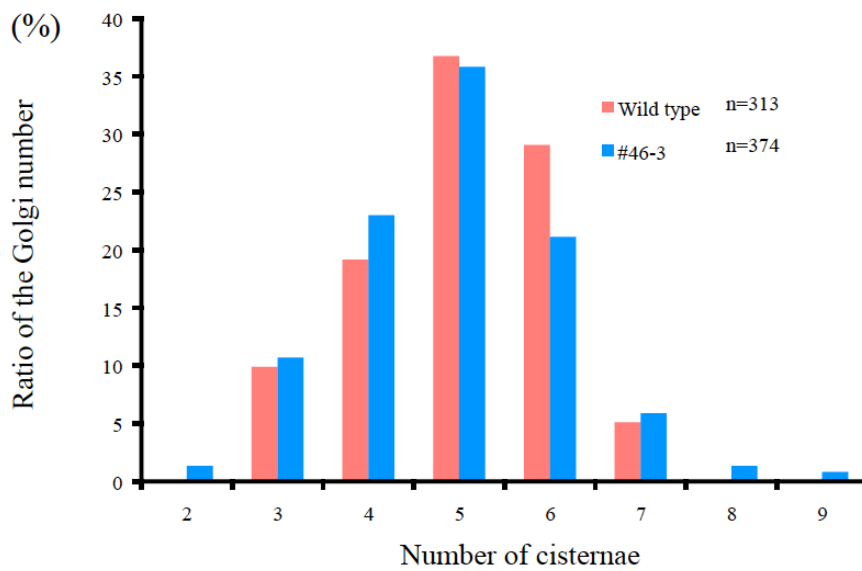


Figure 15. Comparison of the cisternal number of the Golgi between the wild type and the #46-3 mutant.

Histograms showing the cisternal number distribution in individual Golgi stacks.

Generation	Line	Golgi phenotype			
		Normal		Abnormal	
		Number	Ratio (%)	Number	Ratio (%)
F1	1	16	100	0	0
F2	1	13	81.2	3	18.8
	4	14	78.6	3	21.4
	5 (1)	14	87.5	2	12.5
	5 (2)	12	75	4	25
	6 (1)	13	81.2	3	18.8
	6 (2)	6	50	6	50
	6 (3)	12	85.7	2	14.3
	7	15	88.2	2	11.8
	8 (1)	17	70.8	7	29.2
	8 (2)	20	87	3	13
	9	13	68.4	6	31.6
	10 (1)	10	58.8	7	41.2
	10 (2)	15	83.3	3	16.7
	11 (1)	15	75	5	25
	11 (2)	13	72.2	5	27.8
	12 (1)	19	64.3	5	35.7
	12 (2)	9	71.4	2	28.6
	12 (3)	16	76.2	5	23.8
	12 (4)	15	75	5	25
	14 (1)	11	61.1	7	38.9
	14 (2)	17	88.2	2	11.8
	14 (3)	15	75	5	25
	15 (1)	13	61.9	8	38.1
15 (2)	19	82.6	4	17.4	
15 (3)	19	86.4	3	13.6	

Figure 16. The #46-3 mutation is recessive to the wild type.

Segregation of the F2 population indicates that the #46-3 mutation is recessive mutation.

	Marker		Ratio	Average
Chromosome 1	F16J7-TRB	SSLP	3/20	1.10
	CIW1	SSLP	2/20	1.10
	NGA111	SSLP	3/20	1.05
Chromosome 2	CIW2	SSLP	6/20	0.80
	T20D161	CAPS	3/20	1.40
	GBF3	CAPS	3/20	1.20
Chromosome 3	NGA172	SSLP	10/20	0.50
	G4711	CAPS	8/20	0.60
	NGA6	SSLP	10/20	0.70
Chromosome 4	JV30/31	SSLP	11/20	0.50
	CIW7	SSLP	10/20	0.60
	NGA1107	SSLP	7/20	0.80
Chromosome 5	NGA249	SSLP	5/20	1.00
	CIW9	SSLP	6/20	0.85
	MBK-5	SSLP	3/20	1.10

Figure 17. Rough map.

To generate a mapping population, the #46-3 mutant was crossed with Landsberg *erecta*. The genomic DNA of F2 plants exhibiting the abnormal phenotype was roughly mapped with SSLPs and CAPSs markers. The high ratio is showed in position of JV30/31, upper arm of chromosome 4 markers.

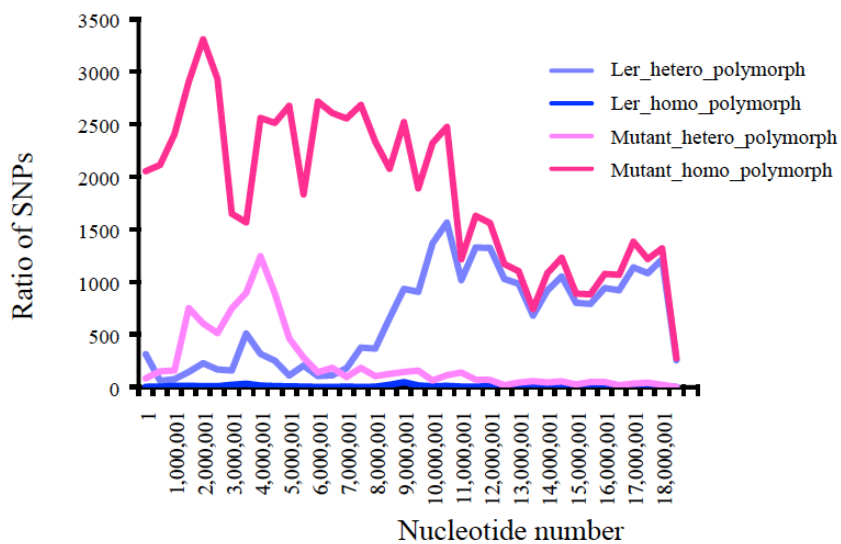


Figure 18. Linkage analysis using a next-generation DNA sequencer.

The candidate region containing the mutation was analyzed by NGS. The results of these analyses nailed down the causal mutation on the upper arm of the chromosome 4 at 1-5.5 Mbp interval by SNP calling. The high ratio is concentrated in position of JV30/31, upper arm of chromosome 4.

Gene	Gene Symbol	Transcript	Consequence	Exon Number	Position in cDNA	Position in Protein	Amino Acid Change
AT4G00500	AT4G00500	AT4G00500.2	SYNONYMOUS CODING	3	1057-1057	280-280	R->R
AT4G00500	AT4G00500	AT4G00500.1	SYNONYMOUS CODING	4	1080-1080	280-280	R->R
AT4G01210	AT4G01210	AT4G01210.1	INTRONIC				
AT4G01680	MYB55	AT4G01680.1	3PRIME_UTR	3	1327-1327		
AT4G01680	MYB55	AT4G01680.3	3PRIME_UTR	4	1221-1221		
AT4G01680	MYB55	AT4G01680.2	3PRIME_UTR	3	1199-1199		
AT4G02410	AT4G02410	AT4G02410.1	NON_SYNONYMOUS_CODING	1	1272-1272	410-410	R->Q
AT4G02750	AT4G02750	AT4G02750.1	NON_SYNONYMOUS_CODING	1	448-448	150-150	E->K
AT4G03745	AT4G03745	AT4G03745.1	EXONIC	1			
			INTERGENIC				
AT4G04410	AT4G04410	AT4G04410.1	EXONIC	1			
			INTERGENIC				
AT4G04910	NSF	AT4G04910.1	NON_SYNONYMOUS_CODING	11	1220-1220	374-374	D->N
AT4G04925	AT4G04925	AT4G04925.1	3PRIME_UTR	1	478-478		
AT4G05390	ATRFNR1	AT4G05390.2	SYNONYMOUS CODING	6	1216-1216	344-344	Q->Q
AT4G05390	ATRFNR1	AT4G05390.1	SYNONYMOUS CODING	5	1288-1288	372-372	Q->Q
			INTERGENIC				
AT4G06477	AT4G06477	AT4G06477.1	EXONIC	1			
			INTERGENIC				
			INTERGENIC				
AT4G06538	AT4G06538	AT4G06538.1	EXONIC	1			
AT4G06546	AT4G06546	AT4G06546.1	EXONIC	1			
			INTERGENIC				
			INTERGENIC				
			INTERGENIC				
AT4G06609	AT4G06609	AT4G06609.1	EXONIC	1			
AT4G06609	AT4G06609	AT4G06609.1	EXONIC	1			
AT4G06656	AT4G06656	AT4G06656.1	EXONIC	1			
AT4G06660	AT4G06660	AT4G06660.1	EXONIC	1			
			INTERGENIC				
AT4G08030	AT4G08030	AT4G08030.1	EXONIC	1			
AT4G08053	AT4G08053	AT4G08053.1	EXONIC	1			
AT4G08099	AT4G08099	AT4G08099.1	EXONIC	1			
AT4G08470	MEKK3	AT4G08470.1	SYNONYMOUS CODING	2	689-689	223-223	K->K
AT4G08598	AT4G08598	AT4G08598.1	EXONIC	1			
AT4G08940	AT4G08940	AT4G08940.1	SYNONYMOUS CODING	1	967-967	315-315	K->K
AT4G12640	AT4G12640	AT4G12640.1	STOP_GAINED	3	744-744	216-216	R->Stop

Figure 19. Three genes are predicted to be missense mutation.

From results in the rough map and the linkage analysis by NGS, only 3 are predicted to be non-silent in open-reading frames (yellow highlighted). They are in the loci At4g04910, At4g02410, and At4g02750.

Gene name	Nucleotide number	Amino Acid Change	Gene annotation
At4g02410	1060882	Arg>Gln	Concanavalin A-like lectin protein kinase family protein
At4g02750	1223014	Glu>Lys	Tetratricopeptide repeat (TPR)-like superfamily protein
At4g04910	2492290	Asp>Asn	<i>N</i> -ethylmaleimide sensitive factor

Figure 20. Candidate genes in the #46-3 mutant.

3 non-silent mutation are in the loci At4g02410, At4g02750, and At4g04910, which were annotated to encode L-type lectin-like protein kinase 1 (AtLPK1), tetratricopeptide repeat (TPR)-like superfamily protein, and *N*-ethylmaleimide-sensitive factor (NSF), respectively.

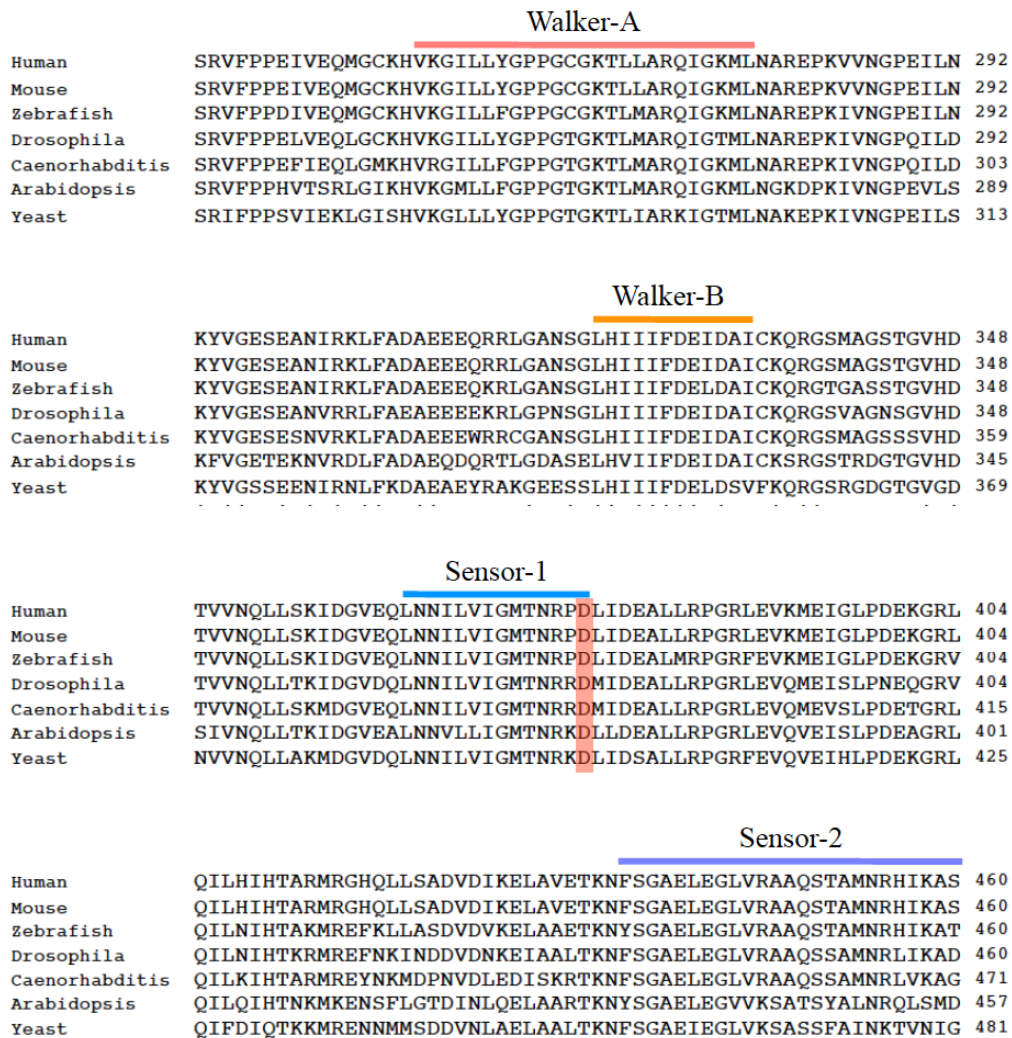


Figure 21. Alignment of the amino acid sequences of NSF.

Sequence alignment of a part of the D1 domain of NSF among different eukaryotic species is shown. Note that the sequence around the position D374 of Arabidopsis (red colored) is highly conserved.

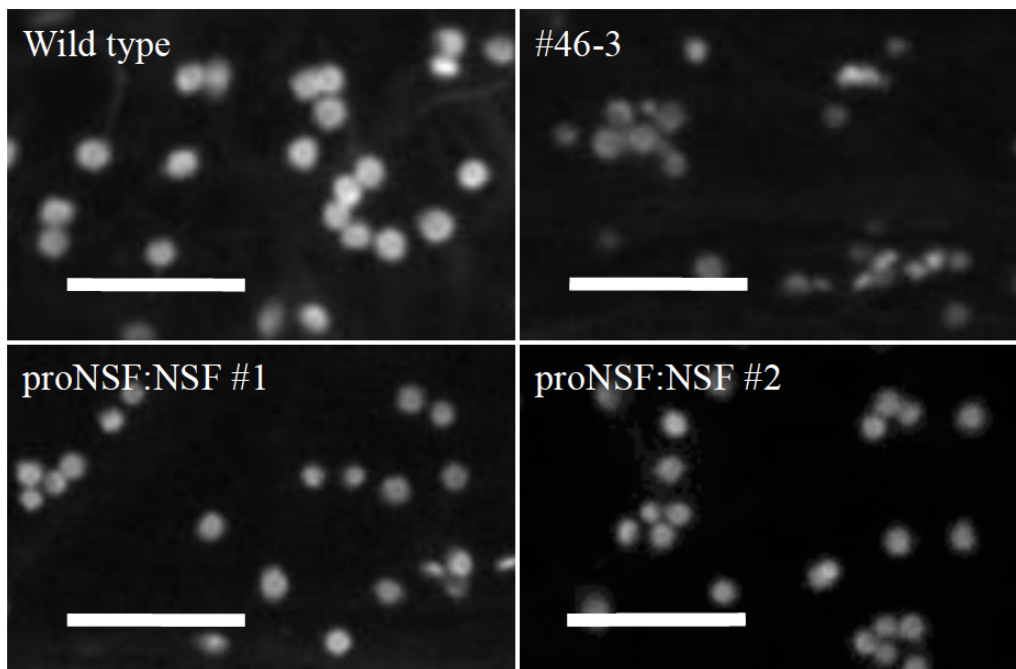


Figure 22. The genomic DNA of *NSF* complements the phenotype of abnormal Golgi morphology in the #46-3 mutant.

Confocal optical sections of epidermal cells of third-leaf-petioles in two independent T2 seedlings, which express the whole sequence of *NSF* in the #46-3 background. Scale bar, 5 μ m.

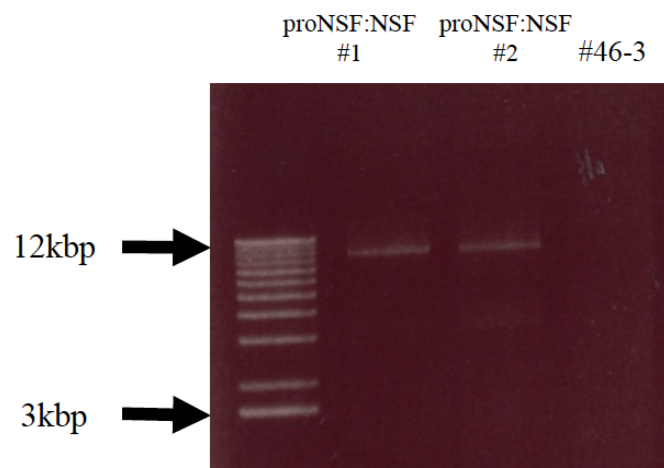


Figure 23. Full length genomic DNA of the *NSF* gene is introduced into the #46-3 mutant.

Genotyping using a primer set of the sequence both vector pHGW and *NSF* gene.

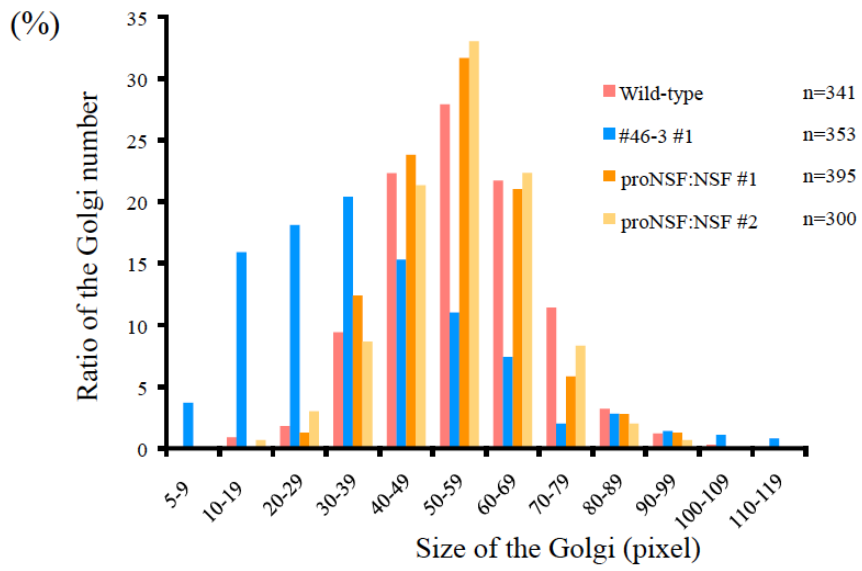
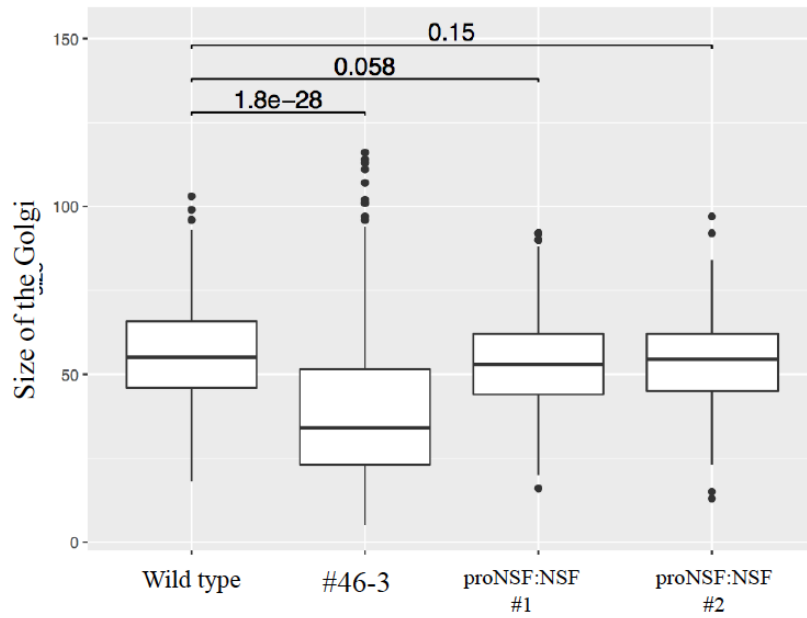
A**B**

Figure 24. Comparison of the Golgi size between the #46-3 mutant and independent two lines of the complementation lines.

- (A) Histograms showing the Golgi size distribution. The Golgi size in 10 petiole cells were measured with ImageJ software.
- (B) Statistic analysis of the histograms in (A). The horizontal line in each box represents the median value of the distribution. The boundaries of a box represent the lower and upper quartile values. The whiskers extending vertically from the upper and lower portions of each box represent the extent of the rest of the data. Numbers denote p values based on Welch's test.

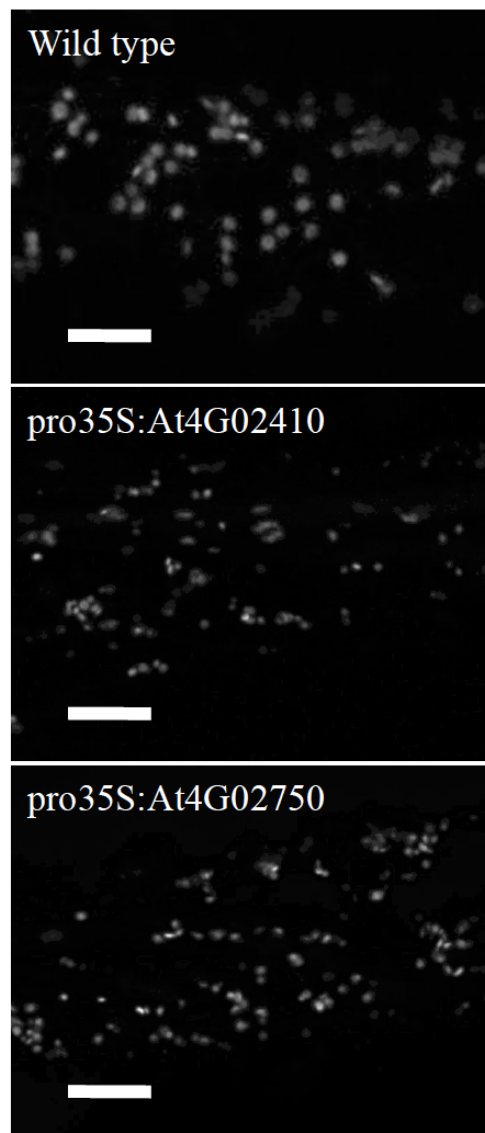
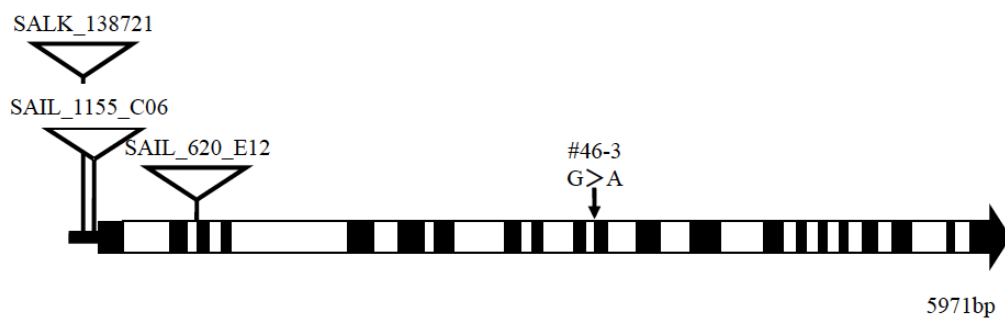


Figure 25. The cording sequence of At4g02410 and At4g02750 do not complement the phenotype of abnormal Golgi morphology in the #46-3 mutant.

Confocal optical sections of epidermal cells of third-leaf-petioles in each T1 seedling expressing the CDS of the two candidate genes in the #46-3 background. Scale bar, 5 μm .



Line name	Insertion site	Nucleotide number	Homozygous plant
SALK_091598/SALK_138721	5' UTR	2495839	viable
SAIL_1155_C06	5' UTR	2495824	lethal
SAIL_620_E12	3 rd exon	2495008	lethal

Figure 26. Three lines containing T-DNA insertions at the *NSF* gene.

T-DNA was inserted in the 5' UTR both in SALK_091598/SALK_138721 and in SAIL_1155_C06 and in the third exon in SAIL_620_E12, respectively. Establishment a homozygous line of SALK_091598/SALK_138721 but not for SAIL_1155_C06 and SAIL_620_E12, probably because the complete knockout of *NSF* is lethal.

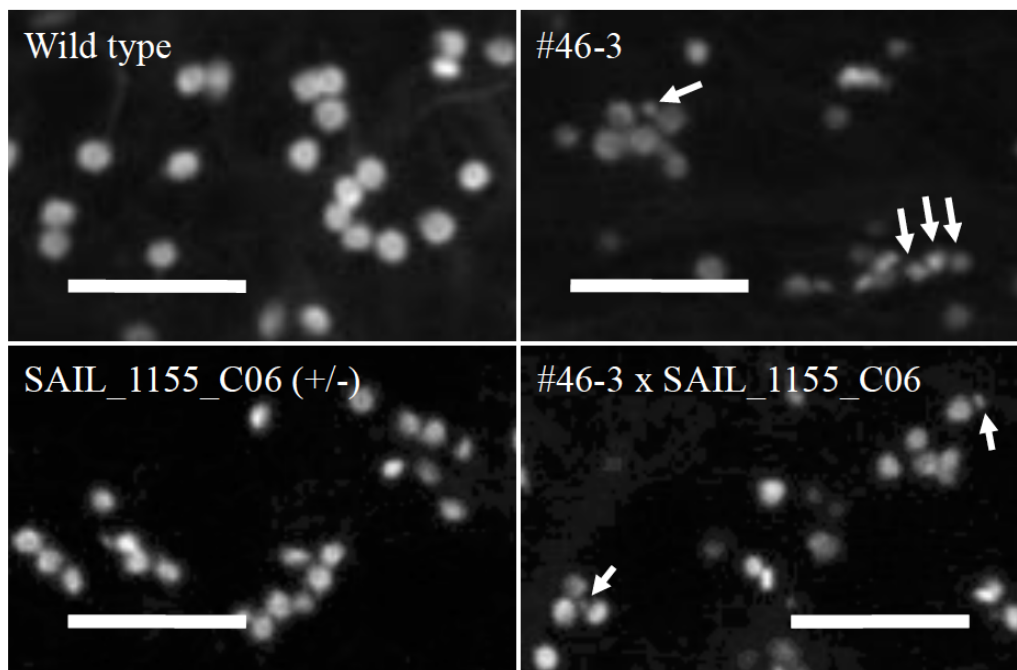
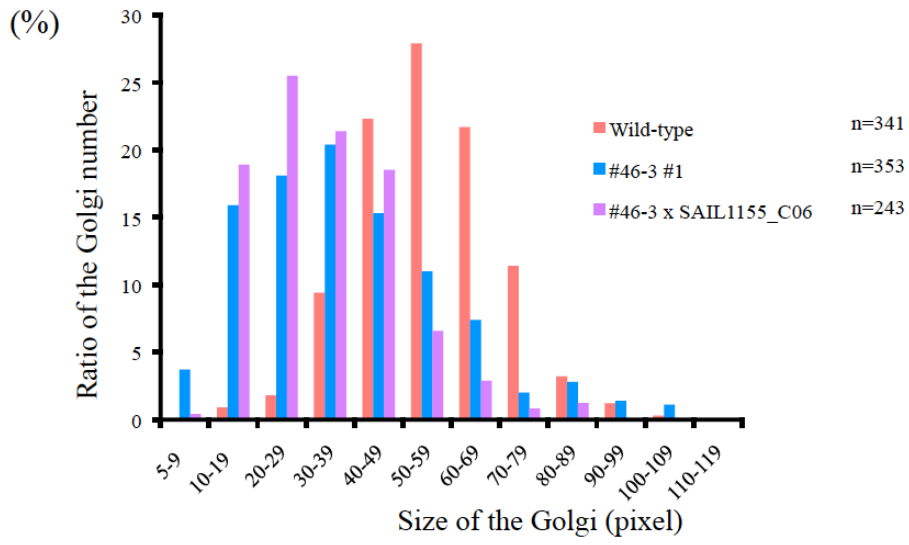


Figure 27. The Golgi of the #46-3/SAIL_1155_C06 heterozygous line shows the abnormal phenotype.

Confocal optical sections of epidermal cells of third-leaf-petioles in the #46-3/SAIL_1155_C06 heterozygous seedlings. Arrows indicate small Golgi. Scale bar, 5 μ m.

A



B

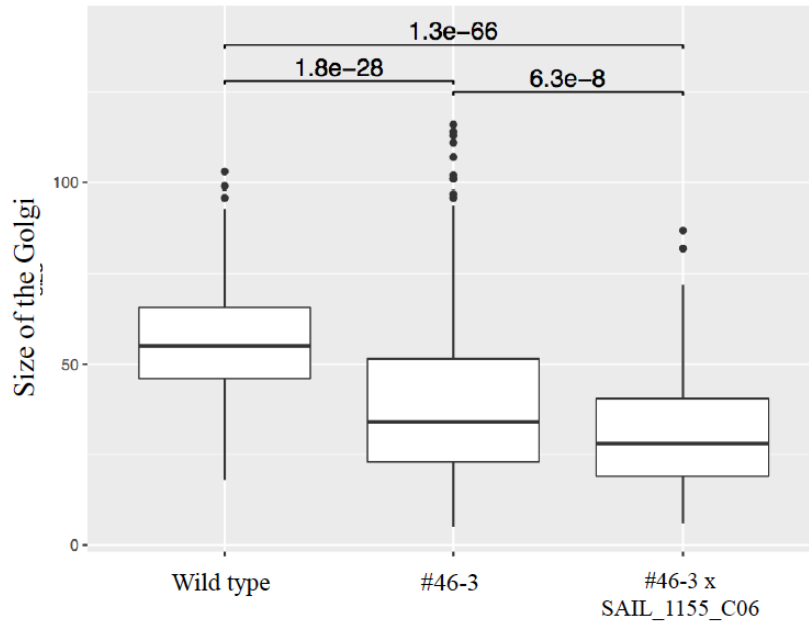


Figure 28. Comparison of the Golgi size between the #46-3 mutant and #46-3/SAIL_1155_C06 heterozygous line.

(A) Histograms showing the Golgi size distribution.

(B) Statistic analysis of the histograms in (A). Numbers denote p values based on Welch's test.

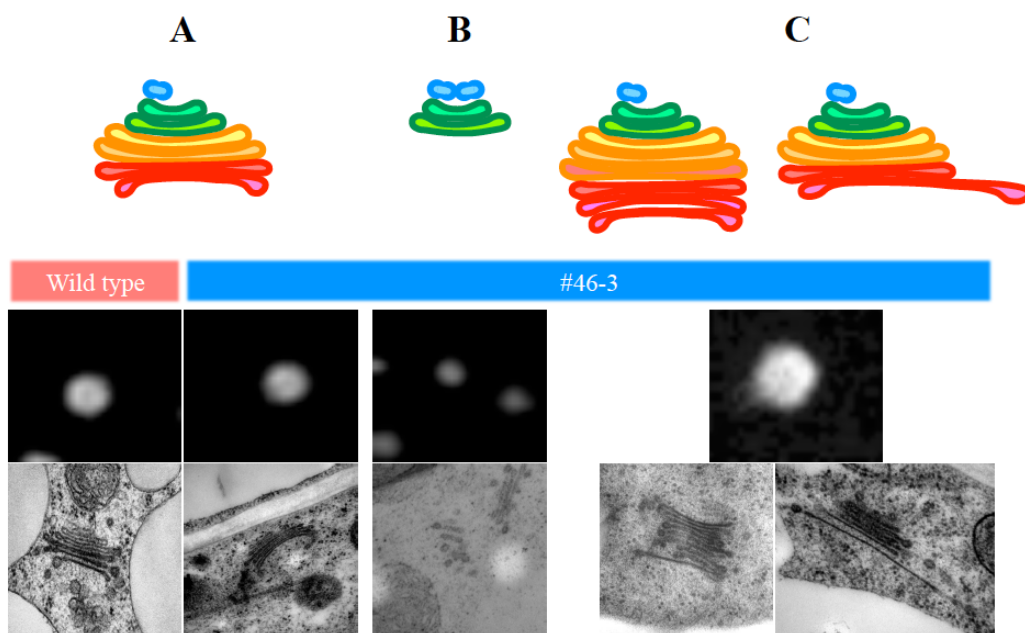


Figure 29. Model of the Golgi phenotypic changes in the #46-3 mutant.

- (A) Normal Golgi in wild type and in the #46-3 mutant.
- (B) Small Golgi observed under confocal microscopy and decreasing the cisternal numbers per Golgi stack showed under electron microscopy in the #46-3 mutant is caused by delay of COPII vesicle disassembly on *cis*-most cisternae.
- (C) Large Golgi observed under confocal microscopy, and increasing the cisternal numbers and the *trans*-most cisternal sizes per Golgi stack under electron microscopy is caused by delay of COPIb vesicle disassembly on medial/*trans* cisternae.

CHAPTER 3

GENERAL DISCUSSION AND PERSPECTIVES

In this study, I attempted to screen and isolate abnormal Golgi morphological mutant designated #46-3 and identified as the responsible gene, *NSF* in *Arabidopsis thaliana*. Thereby, I demonstrated that missense mutation D374N caused pleiotropic Golgi phenotypes in the #46-3 mutant. NSF is one of the most general factors of membrane fusion in eukaryotes (Figure 1). Since it has been well investigated for its function especially in yeast and animals. A dominant negative mutant of *S. cerevisiae SEC18* was exhibited accumulation of a membranous tubular structure (Steel et al., 2000). In zebrafish *Danio rerio* it was showed that the NSF was needed for pigmentation of retinal pigment epithelium (Hanovice et al., 2015). On the other hand, in *Drosophila melanogaster* a neuro-paralytic lethal comatose mutation of *NSF* gene revealed that NSF was particularly required during developmental stage in their life (Pallanck et al., 1995; Sanyal and Krishnan, 2001). In human NSF knockdown suggested a potential role of the NSF in the pathophysiology of autism (Iwata et al., 2014).

Each NSF protomer makes up itself hexamer with a total molecular mass of -500 kDa, constituting three domains including one N terminal domain and two D domains.

NSF-N domains are associated with adapter such as SNAP with electric interaction (Zhao et al., 2015). On the other hand, NSF has two ATPase domains that the D1 domains are responsible for the majority of the ATPase activity whereas the D2 domains are responsible for hexamarization of themselves, respectively. NSF-D1

domain has several characteristic motifs (Neuwald, 1999; Neuwald et al., 1999).

Especially, Motif of Walker-A, Walker-B, sensor-1, sensor-2 and arginine fingers have been investigated to be important for ATPase activity (Datal et al., 2004; Hanson and Whiteheart, 2005; Matveeva et al., 1997; Ogura et al., 2004; Steel et al., 2000) (Figure 21).

To date, the membrane fusion and disassembly process was clarified with an advantage of recent single-particle EM technique without X-ray crystallography (Cheng, 2015; Cheng et al., 2015). In fact, crystal structures of NSF-N domain and NSF-D2 domain have been already obtained, respectively (Yu et al., 1998, 1999). Additionally, crystal structures of the SNARE complex and SNAP/sec17 (yeast homolog) have also elucidated (Rice and Brunger, 1999; Sutton, et al., 1998). Although, crystal structure of the NSF-D1 domain has been not veiled yet. At last, Zhao et al. revealed that the structure of not only NSF-D1 domain but also structural difference between ATP- and ADP-bound NSF with a clear asymmetric feature implied conformational changes due to ATP hydrolysis (2015). Additionally, it was also suggested how the NSF formed 20S complex (SNARE-SNAP-NSF binding) and it disassembled SNARE-SNAP complex (Ryu et al., 2016; Zhao and Blunger, 2016). Now, several working models are proposed how to disassemble in mechanical detail such as distributive, processive or global disassembly (Ryu et al., 2016).

Exceptionally, it has been found that as a binding partner with NSF except SNAP-SNARE complex, AMPA receptors, a class of postsynaptic ionotropic glutamate receptors (Haas, 1998; Lin and Sheng, 1998), and β -arrestin-1, a peripheral membrane

protein also involved in the internalization of many G-protein-coupled receptors (Lefkowitz, 1998; McDonald et al., 1999). These examples indicate that NSF has some functions except ATP-dependent hydrolysis in membrane fusion and disassembly. Indeed, ATPase-deficient *comatose* mutants are displayed lethal phenotype in *Drosophila*, but the Golgi reassembly could sustain to from mitotic Golgi fragments *in vitro* (Pallanck et al., 1995).

A meaningful mutagenesis experiments demonstrated that the NSF(E329Q), ATP binding site mutagenesis caused reduction of NSF-dependent transport activity (Whiteheart et al., 1994) and disrupted Golgi morphology in HeLa cells (Datal et al., 2004; Zhao et al., 2010; Fan et al., 2017). These reports revealed that NSF-D1 domain had ability of not only primary ATP hydrolysis but also alteration of Golgi morphology. Interestingly, Fan et al. demonstrated that NSF knockdown abolished exocytosis of transferrin receptor (TfR) and altered Golgi ribbon structure, but it had virtually no effect on cell viability and constitutive traffic as monitored by vesicular stomatitis virus glycoprotein G (VSVG) trafficking in HeLa cells (2017). Therefore, it is possible that differential requirement of NSF activity for different trafficking pathways in endomembrane system depending the organism and their cell types.

NSF phylogenetically belongs to the “classic clade” of AAA+ members (Erzberger and Berger, 2006). CDC48 (yeast homolog) and valosin-containing protein (VCP/p97, mammalian homolog) as a closest homolog to NSF and of course, CDC48/VCP/p97

also belongs to the “classic clade” AAA+ (Feiler et al., 1995). The function of CDC48 has been studied to be involved in ubiquitin-proteasome system and in endoplasmic reticulum-associated degradation (ERAD), and in plants too (Bègue et al., 2017). Both NSF and CDC48/VCP/p97 share a common domain structure; consisting of two ATPase rings (generally so-called Type II AAA+). It was demonstrated that NSF(E329Q) disrupted the Golgi ribbon but not affect the ER whereas the p97(E578Q) perturbed the ER but not affect the Golgi ribbon in mammalian cells (Datal et al., 2004; Rabouille et al., 1995). It is indicated that not only function but also requirement of NSF and CDC48/VCP/p97 was unambiguously different in the secretory pathway.

In *Arabidopsis*, *NSF* is a single-copy gene as in other eukaryotes (Sanderfoot et al., 2000). In contrast, based on phylogenetic analysis in plants, many SNARE species have been characterized and classified among the green plants (Sanderfoot, 2007). In the Golgi apparatus of *A. thaliana* of cultured cells, nine SNARE molecules were mapped; two Qa-SNAREs, AtSYP31 and AtSYP32; four Qb-SNAREs, AtGOS11, AtGOS12, AtMEMB11, and AtMEMB12; two Qc-SNAREs, AtBS14a and AtBS14b; and one R-SNARE, AtVAMP714 (Uemura et al., 2004). Furthermore, El-Kasmi et al. demonstrated that in *Arabidopsis* mutant of R-SNARE SEC-22, which localize to the ER and *cis*-Golgi, showed to cause male sterility by reciprocal crosses and Golgi fragmentation during pollen developmental stage by electron microscopy (2011). As showed in this study, both in SAIL_620_E12 and SAIL_1155_C06, T-DNA insertion mutants, homozygous plants were lethal. It was implied that they were male sterility

because of never available their progeny when their pollen were reciprocally crossed. I presume that intra-Golgi trafficking is active during pollen developmental stage and membrane fusion event is accelerated, that SNAREs and NSF are significantly required for pollen maturing and maintenance of Golgi morphology in pollen.

Additionally, it is known as a plant-specific phenomenon, formation of the cell plate is processed after cytokinesis is occurred. In animal and fungal cells, cytokinesis proceeds with an actomyosin ring contracting. In contrast, in plant cytokinesis a number of vesicles delivered along a cytoskeleton to the plane of cell division. By the way, It is not entirely revealed that how the Golgi is inherit when cell division. Of course, NSF is supposed to hardly work at that time with SNAREs such as KNOLLE, cytokinesis-specific Qa-SNARE (Jürgens et al., 2015; Lauber et al., 1997; Lukowitz et al., 1995) during cytokinesis including pollen mitosis.

What controls the cisternal numbers in the Golgi? The alteration of Golgi morphology attributed to increasing/decreasing cisternal number of the Golgi in the #46-3 mutant (in this study). The mechanisms controlling the cisternal number per Golgi stack are unknown, however it has been proposed that a change in influx/efflux ratio within the Golgi is one of important factors for maintenance of organelle size (Sengupta and Linstedt, 2011). Therefore, it is considered that transport velocity is one of important factor for cisternal increasing. Because during flagella regeneration the Golgi produced one *cis*-most cisterna for 15 seconds in *S. dubia* while it generated that for 2-4 minutes in *A. thaliana* (Donohoe et al., 2013). It is suggested that COPII-coated vesicle budding

on the ERES and cisternal assembly are faster than COPI-coated vesicle generation on the cisternal rims in *S. dubia*. As mentioned above, without doubt, it was clearly demonstrated that the membranes in the Golgi are in a very dynamic equilibrium by the cisternal maturation and retrieval of COPI-coated vesicles (Ishii et al., 2016; Losev et al., 2006; Matsuura-Tokita et al., 2006; Papanikou et al., 2015). Hence, I consider that in the #46-3 mutant observed abnormal Golgi stacks consisting of increased numbers of cisternae is due to hindrance of the equilibrium in intra-Golgi trafficking because disassembly of COPI-coated vesicles are delayed.

Previously, it was experimented that in mammalian cells the increases in the size of *trans*-cisternae resulted in block the exit of protein cargo from the Golgi (Ladinsky et al., 2002). Subsequently, recent ultrastructural study also demonstrated that the depletion of Rab6, mammalian small GTPase localized *trans*-cisternae, caused the significant increases in cisternal number and accumulation of COPI-coated vesicles at *trans*-Golgi (Storrie et al., 2012). Additionally, the *arf1Δ* mutation (partially depleting the Arf GTPase) showed to mature the Golgi more slowly and less frequently, but not to abolish the maturation kinetics (Bhave, et al., 2014). It is suggested that the Golgi size depending on their cisternal number and equilibrium of intra-Golgi trafficking is controlled by not only COPI proteins but also Arf GTPase. Then, *in planta* it showed that Arabidopsis Qb-SNARE MEMB11 (membrin, mammalian homolog) mainly localized to *cis*-Golgi interacted with Arf1 from biochemical assay and live imaging (Marais et al., 2015). It is expect to get more information how SNAREs and small GTPase are involved in maintenance of Golgi morphology in not only cultured

cells but also whole plants.

Ultimately, I have one provocative question. Why does the #46-3 mutant show pleiotropic Golgi phenotypes but not uniform? I speculate that the individual Golgi stack has each unique function alternatively specialized such as glycosylation and phosphorylation. Otherwise, the NSF possibly has plant-specific functions except ATP-dependent hydrolysis in membrane fusion events.

I believe that the discoveries in this study will contribute to reveal the molecular mechanism to form and maintain the Golgi morphology by the NSF; it would be realized soon with an advance in state-of-the art live imaging techniques.

EXPERIMENTAL PROCEDURES

Plant materials and growth conditions

For wild-type plants of *A. thaliana*, ecotypes Colombia-0 (Col-0) and Landsberg *erecta* were used in this study. Seeds of the transgenic plant of *A. thaliana* (Col-0) expressing ERD2-GFP (Boevink et al., 1998; Takeuchi et al., 2000, 2002) (named A21) were mutagenized by treatment with 0.3% ethyl methanesulfonate (EMS) for 16 h. A21 and mutagenesis M2 seeds are gifts from Ms. Keiko Shoda. ST-mRFP expressing plant is provided from Dr. Tomohiro Uemura. T-DNA insertion mutants, SALK_091598/SALK_138721, SAIL_1155_C06 and SAIL_620_E12 were obtained from the Arabidopsis Biological Resource Center (Columbus, OH, USA). Mutants were backcrossed three times with the wild-type Col-0. Surviving seedlings were individually grown up and subjected to self-pollination to establish M2-generation lines. M2 seeds were sown on MS medium [1 x MS salt, 1% sucrose, vitamin mix and 0.2% agar], vernalized in the dark at 4°C for 4 days, and grown at 23°C under continuous light. Selection media contained glufosinate ammonium salt (BASTA; final concentration 7.5 µg/ml) or kanamycin (50 µg/ml) for T-DNA insertion lines and hygromycin (25 µg/ml) for complementation lines.

Plasmid Constructions

To isolate the *NSF* gene under its own promoter (*proNSF:NSF*), a genomic fragment was amplified by PCR using a primer set (5'-

AACCAATTCAGTCGACTCGGAGAAAAGAGGGCAAGT-3' and 5' AAGCTGGGTCTAGATAATGTTGTGCGAAGTGAGAGTC-3'). Gateway pENTR 1A dual selection vector (Thermo Fisher Scientific/Invitrogen, Waltham, MA, USA) was amplified by PCR using a primer set (5'-AACCAATTCAGTCGAC-3' and 5'-AAGCTGGGTCTAGATA-3'). After treatment of Gateway pENTR 1A with restriction enzymes *SalI* and *EcoRV*, the genomic fragment was cloned into the vector pENTR 1A and recombined into pHGW (Karimi et al., 2002) by LR Clonase II (Thermo Fisher Scientific/Invitrogen). Transformed lines were obtained with a floral dip procedure (Clough and Bent, 1998).

Isolation of the #46-3 mutant and genetic analysis

M2 ERD2-GFP seeds were grown for 16 days and observed under a confocal microscope. A homozygous mutant line named #46-3, showing abnormal morphology of the Golgi, was crossed with Landsberg *erecta* to generate a F2 mapping population. *A. thaliana* ecotype-specific markers of simple sequence length polymorphisms and cleaved amplified polymorphic sequences were used for rough mapping on 20 individuals showing the abnormal Golgi phenotype.

For genome-sequencing, bulked F2 seedlings exhibiting the mutant phenotype were selected and purified genome is followed several steps; (1) Preparation of genomic DNA samples for deep-sequencing; extracted DNA were fragmented by ultrasonic and. Samples were added 'A' bases to the end of the DNA fragments and ligated adapters to that. Then, samples were enriched the adapter-modified DNA fragments by PCR and

confirmed the quality of genomic DNA library after purified ligation products. (2) Deep-sequencing, (3) SNP data acquisition against the reference Col-0 genome, (4) Linkage analysis by the index of enrichment of homozygous SNPs, (5) SNP filtering and SNPs calling, a modified method from Uchida et al. (2011) was used. SNPs calling was performed under Strand NGS software (Strand Life Sciences).

Confocal microscopy

For single-color imaging, transgenic plants were visualized under an Olympus IX81 fluorescence microscope equipped with a confocal laser-scanning unit (CSU10, Yokogawa Electronic, Tokyo, Japan) and images were acquired by a CCD camera ORCA-R2 (Hamamatsu Photonics, Hamamatsu, Japan). Dual-color imaging was carried out with a LSM780 confocal microscope (Zeiss, Jena, Germany). The central regions of petioles 16 days after germination were mounted with water on glass slides. Images were processed and analyzed with ImageJ 1.49i (National Institute of Health, Bethesda, MD, USA). For size measurement of the Golgi, image processing was carried out by Otsu's method with ImageJ 1.49i. (Otsu, 1979).

Electron microscopy

16-day-old petioles of seedlings (wild type and #46-3) were rapidly frozen in a high-pressure freezer (HPM010; Bal-Tec). Frozen samples were transferred to 2% osmium tetroxide in anhydrous acetone that had been precooled with liquid nitrogen. Samples were maintained at -80°C for 7 days, at -20°C for 2 h, at 4°C for 2 h, and then

at room temperature for 2 h. After several washes with anhydrous acetone, samples were embedded in Spurr's resin (Nisshin EM). Ultrathin sections (thickness 60-80nm) were cut for electron microscopic observation after thin sections (thickness 1 μ m) were cut for light microscopic observation to confirm where was the cell type. Every time cutting ultrathin section, thin sections were also cut because of avoidance same Golgi included within the section. Ultrathin sections then stained with uranyl acetate and lead citrate, and observed under a transmission electron microscope (JEM-1010; JEOL).

REFERENCES

Appenzeller-Herzog, C. and Hauri, H.P. 2006. The ER-Golgi intermediate compartment (ERGIC): in search of its identity and function. *J. Cell Sci.* **119**: 2173-2183.

Arabidopsis Genome Initiative. 2000. Analysis of the genome sequence of the flowering plant *Arabidopsis thaliana*. *Nature* **408**: 796-815.

Austin, R.S., Vidaurre, D., Stamatiou, G., Breit, R., Provar, N.J., Bonetta, D., Zhang, J., Fung, P., Gong, Y., Wang, P.W., McCourt, P. and Guttman, D.S. 2011. Next-generation mapping of Arabidopsis genes. *Plant J.* **67**: 715-725.

Barlowe, C. and Schekman, R. 1993. *SEC12* encodes a guanine-nucleotide-exchange factor essential for transport vesicle budding from the ER. *Nature* **365**: 347-349.

Bar-Peled, M., Conceicao, A., Frigerio, L. and Raikhel, N.V. 1995. Expression and Regulation of *aERD2*, a Gene Encoding the KDEL Receptor Homolog in Plants, and Other Genes Encoding Proteins Involved in ER-Golgi Vesicular Trafficking. *Plant Cell* **7**: 667-676.

Becker, B., Bölinger, B. and Melkonian, M. 1995. Anterograde transport of algal scales through the Golgi complex is not mediated by vesicles. *Trends Cell Biol.* **5**: 305-307.

Bègue, H., Jeandroz, S., Blankchard, C., Wendehenne, D. and Rosnoblet, C. 2017. Structure and functions of the chaperone-like p97/CDC48 in plants. *Biochim. Biophys. Acta.* **1861**: 3053-3060.

Bell, C.J. and Ecker, J.R. 1994. Assignment of 30 microsatellite loci to the linkage map of *Arabidopsis*. *Genomics* **19**: 137-144.

Bhave, M., Papanikou, E., Iyer, P., Pandya, K., Jain, B.K., Ganguly, A., Sharma, C., Pawar, K., Austin, J.II., Day, K.J., Rossanese, O.W., Glick, B.S, and Bhattacharyya, D.

2014. Golgi enlargement in Arf-depleted yeast cells is due to altered dynamics of cisternal maturation. *J. Cell Sci.* **127**: 250-257.

Bi, X., Mancias, J.D. and Goldberg, J. 2007. Insights into COPII coat nucleation from the structure of Sec23•Sar1 complexed with the active fragment of Sec31. *Dev. Cell* **13**: 635-645.

Block, M.R., Glick, B.S., Wilcox, C.A., Wieland, F.T. and Rothman, J.E. 1988. Purification of an *N*-ethylmaleimide-sensitive protein catalyzing vesicular transport. *Proc. Natl. Acad. Sci. U. S. A.* **85**: 7852-7856.

Boevink, P., Oparka, K., Santa Cruz, S., Martin, B., Betteridge, A. and Hawes, C. 1998. Stacks on tracks: the plant Golgi apparatus traffics on an actin/ER network. *Plant J.* **15**: 441-447.

Bonfanti, L., Mironov, A.A. Jr., Martínez-Menárguez, J.A., Martella, O., Fusella, A., Baldassarre, M., Buccione, R., Geuze, H.J., Mironov, A.A. and Luini, A. 1998. Procollagen traverses the Golgi stack without leaving the lumen of cisternae: evidence for cisternal maturation. *Cell* **95**: 993-1003.

Boulaflous, A., Faso, C. and Brandizzi, F. 2008. Deciphering the Golgi apparatus: from imaging to genes. *Traffic* **9**: 1613-1617.

Chen, J., Stefano, G., Brandizzi, F. and Zheng, H. 2011. *Arabidopsis* RHD3 mediates the generation of the tubular ER network and is required for Golgi distribution and motility in plant cells. *J. Cell Sci.* **124**: 2241-2252.

Cheng, Y. 2015. Single-Particle Cryo-EM at Crystallographic Resolution. *Cell* **161**: 450-457.

Cheng, Y., Grigorieff, N., Penczek, P.A. and Walz, T. 2015. A primer to single-particle cryo-electron microscopy. *Cell* **161**: 438-449.

Cipriano, D.J., Jung, J., Vivona, S., Fenn, T.D., Brunger, A.T. and Bryant, Z. 2013. Processive ATP-driven substrate disassembly by the *N*-ethylmaleimide-sensitive factor (NSF) molecular machine. *J. Biol. Chem.* **288**: 23436-23445.

Clough, S.J. and Bent, A.F. 1998. Floral dip: a simplified method for *Agrobacterium*-mediated transformation of *Arabidopsis thaliana*. *Plant J.* **16**: 735-743.

Dalton, A.J. 1951. Observations of the Golgi substance with the electron microscope. *Nature* **168**: 244-245.

Dalton, A.J. and Felix, M.D. 1954. Cytologic and cytochemical characteristics of the Golgi substance of epithelial cells of the epididymis—in situ, in homogenates and after isolation. *Am. J. Anat.* **94**: 171-207.

Day, K.J., Staehelin, L.A. and Glick, B.S. 2013. A three-stage model of Golgi structure and function. *Histochem. Cell Biol.* **140**: 239-249.

Dalal, S., Rosser, M.F., Cyr, D.M. and Hanson, P.I. 2004. Distinct roles for the AAA ATPases NSF and p97 in the secretory pathway. *Mol. Biol. Cell* **15**: 637-648.

Dell'Angelica, E.C. 2009. AP-3-dependent trafficking and disease: the first decade. *Curr. Opin. Cell Biol.* **21**: 552-559.

Derby, M.C. and Gleeson, P.A. 2007. New insights into membrane trafficking and protein sorting. *Int. Rev. Cytol.* **261**: 47-116.

Donohoe, B.S., Kang, B.H., Gerl, M.J., Gergely, Z.R., McMichael, C.M., Bednarek, S.Y. and Staehelin, L.A. 2013. *Cis*-Golgi cisternal assembly and biosynthetic activation occur sequentially in plants and algae. *Traffic* **14**: 551-567.

Donohoe, B.S., Kang, B.H. and Staehelin, L.A. 2007. Identification and characterization of COPIa- and COPIb-type vesicle classes associated with plant and algal Golgi. *Proc. Natl. Acad. Sci. U. S. A.* **104**: 163-168.

Dunphy, W.G. and Rothman, J.E. 1985. Compartmental organization of the Golgi stack. *Cell* **42**: 13-21.

El-Kasmi, F., Pacher, T., Strompen, G., Stierhof, Y.D., Müller, L.M., Koncz, C., Mayer, U. and Jürgens, G. 2011. Arabidopsis SNARE protein SEC22 is essential for gametophyte development and maintenance of Golgi-stack integrity. *Plant J.* **66**: 268-279.

Emr, S., Glick, B.S., Linstedt, A.D., Lippincott-Schwartz, J., Luini, A., Malhotra, V., Marsh, B.J., Nakano, A., Pfeffer, S.R., Rabouille, C., Rothman, J.E., Warren, G. and Wieland, F.T. 2009. Journeys through the Golgi--taking stock in a new era. *J. Cell Biol.* **187**: 449-453.

Erzberger, J.P. and Berger, J.M. 2006. Evolutionary relationships and structural mechanisms of AAA+ proteins. *Annu. Rev. Biophys. Biomol. Struct.* **35**: 93-114.

Fan, J., Zhou, X., Wang, Y., Kuang, C., Sun, Y., Liu, X., Toomre, D. and Xu, Y. 2017. Differential requirement for *N*-ethylmaleimide-sensitive factor in endosomal trafficking of transferrin receptor from anterograde trafficking of vesicular stomatitis virus glycoprotein G. *FEBS Lett.* **591**: 273-281.

Faso, C., Boulaflous, A. and Brandizzi, F. 2009. The plant Golgi apparatus: last 10 years of answered and open questions. *FEBS Lett.* **583**: 3752-3757.

Faso, C., Chen, Y.N., Tamura, K., Held, M., Zemelis, S., Marti, L., Saravanan, R., Hummel, E., Kung, L., Miller, E., Hawes, C. and Brandizzi, F. 2009. A missense mutation in the *Arabidopsis* COPII coat protein Sec24A induces the formation of clusters of the endoplasmic reticulum and Golgi apparatus. *Plant Cell* **21**: 3655-3671.

Fasshauer, D., Sutton, R.B., Brunger, A.T. and Jahn, R. 1998. Conserved structural features of the synaptic fusion complex: SNARE proteins reclassified as Q- and R-SNAREs. *Proc. Natl. Acad. Sci. U. S. A.* **95**: 15781-15786.

Feiler, H.S., Desprez, T., Santoni, V., Kronenberger, J., Caboche, M. and Traas, J. 1995. The higher plant *Arabidopsis thaliana* encodes a functional *CDC48* homologue which is highly expressed in dividing and expanding cells. *EMBO J.* **14**: 5626-5637.

Feraru, E., Paciorek, T., Feraru, M.I., Zwiewka, M., De Groot, R., De Rycke, R., Kleine-Vehn, J. and Friml, J. 2010. The AP-3 β adaptin mediates the biogenesis and function of lytic vacuoles in *Arabidopsis*. *Plant Cell* **22**: 2812-2824.

Geldner, N., Anders, N., Wolters, H., Keicher, J., Kornberger, W., Müller, P., Delbarre, A., Ueda, T., Nakano, A. and Jürgens, G. 2003. The *Arabidopsis* GNOM ARF-GEF mediates endosomal recycling, auxin transport, and auxin-dependent plant growth. *Cell* **112**: 219-230.

Glick, B.S. 2000. Organization of the Golgi apparatus. *Curr. Opin. Cell Biol.* **12**: 450-456.

Glick, B.S. and Luini, A. 2011. Models for Golgi traffic: a critical assessment. *Cold Spring Harbor Perspect. Biol.* **3**: a005215.

Glick, B.S. and Malhotra, V. 1998. The curious status of the Golgi apparatus. *Cell* **95**: 883-889.

Glick, B.S. and Nakano, A. 2009. Membrane traffic within the Golgi apparatus. *Annu. Rev. Cell Dev. Biol.* **25**: 113-132.

Glick, B.S. and Rothman, J.E. 1987. Possible role for fatty acyl-coenzyme A in intracellular protein transport. *Nature* **326**: 309-312.

Golgi, C. 1898. Sur la structure des cellules nerveuses. *Arch. Ital. Biol.* **30**: 60-71.

Haas, A. 1998. NSF--fusion and beyond. *Trends Cell Biol.* **8**: 471-473.

Hanovice, N.J., Daly, C.M. and Gross, J.M. 2015. N-Ethylmaleimide-Sensitive Factor b (nsfb) Is Required for Normal Pigmentation of the Zebrafish Retinal Pigment Epithelium. *Invest. Ophthalmol. Vis. Sci.* **56**: 7535-7544.

Hanson, P.I. and Whiteheart, S.W. 2005. AAA+ proteins: have engine, will work. *Nat. Rev. Mol. Cell Biol.* **6**: 519-529.

Hanton, S.L., Bortolotti, L.E., Renna, L., Stefano, G. and Brandizzi, F. 2005. Crossing the divide--transport between the endoplasmic reticulum and Golgi apparatus in plants. *Traffic* **6**: 267-277.

Hawes, C., Osterrieder, A., Hummel, E. and Sparkes, I. 2008. The plant ER-Golgi interface. *Traffic* **9**: 1571-1580.

Hong, W. 2005. SNAREs and traffic. *Biochim. Biophys. Acta.* **1744**: 493-517.

Ishii, M., Suda, Y., Kurokawa, K. and Nakano, A. 2016. COPI is essential for Golgi cisternal maturation and dynamics. *J. Cell Sci.* **129**: 3251-3261.

Ito, Y., Toyooka, K., Fujimoto, M., Ueda, T., Uemura, T. and Nakano, A. 2017. The *trans*-Golgi Network and the Golgi Stacks Behave Independently During Regeneration After Brefeldin A Treatment in Tobacco BY-2 Cells. *Plant Cell Physiol.* **58**: 811-821.

Ito, Y., Uemura, T. and Nakano, A. 2014. Formation and maintenance of the Golgi apparatus in plant cells. *Int. Rev. Cell Mol. Biol.* **310**: 221-287.

Ito, Y., Uemura, T. and Nakano, A. 2018. Golgi entry core compartment functions as the COPII-independent scaffold for ER-Golgi transport in plant cells. *J. Cell Sci.* **131**: jcs203893.

Ito, Y., Uemura, T., Shoda, K., Fujimoto, M., Ueda, T., and Nakano, A. 2012. *cis*-Golgi proteins accumulate near the ER exit sites and act as the scaffold for Golgi regeneration after brefeldin A treatment in tobacco BY-2 cells. *Mol. Biol. Cell* **23**: 3203-3214.

Iwata, K., Matsuzaki, H., Tachibana, T., Ohno, K., Yoshimura, S., Takamura, H., Yamada, K., Matsuzaki, S., Nakamura, K., Tsuchiya, K.J., Matsumoto, K., Tsujii, M., Sugiyama, T., Katayama, T. and Mori, N. 2014. *N*-ethylmaleimide-sensitive factor interacts with the serotonin transporter and modulates its trafficking: implications for pathophysiology in autism. *Mol. Autism* **5**: 33.

Iyer, L.M., Leipe, D.D., Koonin, E.V. and Aravind, L. 2004. Evolutionary history and higher order classification of AAA+ ATPases. *J. Struct. Biol.* **146**: 11-31.

Jackson, C.L. and Casanova, J.E. 2000. Turning on ARF: the Sec7 family of guanine-nucleotide-exchange factors. *Trends Cell Biol.* **10**: 60-67.

Jürgens, G., Park, M., Richter, S., Touihri, S., Krause, C., El Kasmi, F. and Mayer, U. 2015. Plant cytokinesis: a tale of membrane traffic and fusion. *Biochem. Soc. Trans.* **43**: 73-78.

Kang, B.H., Nielsen, E., Preuss, M.L., Mastronarde, D. and Staehelin, L.A. 2011. Electron tomography of RabA4b- and PI-4K β 1-labeled *trans* Golgi network compartments in *Arabidopsis*. *Traffic* **12**: 313-329.

Karimi, M., Inzé, D. and Depicker, A. 2002. GATEWAY vectors for Agrobacterium-mediated plant transformation. *Trends Plant Sci.* **7**: 193-195.

Klumperman, J. 2011. Architecture of the mammalian Golgi. *Cold Spring Harb. Perspect. Biol.* **3**: a005181.

Konieczny, A. and Ausubel, F.M. 1993. A procedure for mapping *Arabidopsis* mutations using co-dominant ecotype-specific PCR-based markers. *Plant J.* **4**: 403-410.

Kurokawa, K., Ishii, M., Suda, Y., Ichihara, A. and Nakano, A. 2013. Live cell visualization of Golgi membrane dynamics by super-resolution confocal live imaging microscopy. *Methods Cell Biol.* **118**: 235-242.

Ladinsky, M.S., Mastronarde, D.N., McIntosh, J.R., Howell, K.E. and Staehelin, L.A. 1999. Golgi structure in three dimensions: functional insights from the normal rat kidney cell. *J. Cell Biol.* **144**: 1135-1149.

Ladinsky, M.S., Wu, C.C., McIntosh, S., McIntosh, J.R. and Howell, K.E. 2002. Structure of the Golgi and distribution of reporter molecules at 20°C reveals the complexity of the exit compartments. *Mol. Biol. Cell* **13**: 2810-2825.

Lauber, M.H., Waizenegger, I., Steinmann, T., Schwarz, H., Mayer, U., Hwang, I., Lukowitz, W. and Jürgens, G. 1997. The *Arabidopsis* KNOLLE protein is a cytokinesis-specific syntaxin. *J. Cell Biol.* **139**: 1485-1493.

Leblond, C.P. and Inoue, S. 1989. Structure, composition, and assembly of basement membrane. *Am. J. Anat.* **185**: 367-390.

Lefkowitz, R.J. 1998. G protein-coupled receptors. III. New roles for receptor kinases and β -arrestins in receptor signaling and desensitization. *J. Biol. Chem.* **273**: 18677-18680.

Lenzen, C.U., Steinmann, D., Whiteheart, S.W. and Weis, W.I. 1998. Crystal structure of the hexamerization domain of N-ethylmaleimide-sensitive fusion protein. *Cell* **94**: 525-536.

Lin, J.W. and Sheng, M. 1998. NSF and AMPA receptors get physical. *Neuron* **21**: 267-270.

Losev, E., Reinke, C.A., Jellen, J., Strongin, D.E., Bevis, B.J. and Glick, B.S. 2006. Golgi maturation visualized in living yeast. *Nature* **441**: 1002-1006.

Luini, A. 2011. A brief history of the cisternal progression-maturation model. *Cell Logist.* **1**: 6-11.

Lukowitz, W., Mayer, U. and Jürgens, G. 1996. Cytokinesis in the Arabidopsis embryo involves the syntaxin-related KNOLLE gene product. *Cell* **84**: 61-71.

Malhotra, V., Orci, L., Glick, B.S., Block, M.R. and Rothman, J.E. 1988. Role of an *N*-ethylmaleimide-sensitive transport component in promoting fusion of transport vesicles with cisternae of the Golgi stack. *Cell* **54**: 221-227.

Marais, C., Wattelet-Boyer, V., Bouyssou, G., Hocquellet, A., Dupuy, J.W., Batailler, B., Brocard, L., Boutté, Y., Maneta-Peyret, L. and Moreau, P. 2015. The Qb-SNARE Memb11 interacts specifically with Arf1 in the Golgi apparatus of *Arabidopsis thaliana*. *J. Exp. Bot.* **66**: 6665-6678.

Marti, L., Stefano, G., Tamura, K., Hawes, C., Renna, L., Held, M.A. and Brandizzi, F. 2010. A missense mutation in the vacuolar protein GOLD36 causes organizational defects in the ER and aberrant protein trafficking in the plant secretory pathway. *Plant J.* **63**: 901-913.

Martinez-Menárguez, J.A., Prekeris, R., Oorschot, V.M., Scheller, R., Slot, J.W., Geuze, H.J. and Klumperman, J. 2001. Peri-Golgi vesicles contain retrograde but not anterograde proteins consistent with the cisternal progression model of intra-Golgi transport. *J. Cell Biol.* **155**: 1213-1224.

Matheson, L.A., Hanton, S.L. and Brandizzi, F. 2005. Traffic between the plant endoplasmic reticulum and Golgi apparatus: to the Golgi and beyond. *Curr. Opin. Plant Biol.* **9**: 601-609.

Matsushima, R., Hayashi, Y., Kondo, M., Shimada, T., Nishimura, M. and Hara-Nishimura, I. 2002. An endoplasmic reticulum-derived structure that is induced under stress conditions in Arabidopsis. *Plant Physiol.* **130**: 1807-1814.

Matsuoka, K., Schekman, R., Orci, L. and Heuser, J.E. 2001. Surface structure of the COPII-coated vesicle. *Proc. Natl. Acad. Sci. U. S. A.* **98**: 13705-13709.

- Matsuura-Tokita, K., Takeuchi, M., Ichihara, A., Mikuriya, K., and Nakano, A. 2006. Live imaging of yeast Golgi cisternal maturation. *Nature* **441**: 1007-1010.
- Matveeva, E.A., He, P. and Whiteheart, S.W. 1997. *N*-Ethylmaleimide-sensitive fusion protein contains high and low affinity ATP-binding sites that are functionally distinct. *J. Biol. Chem.* **272**: 26413-26418.
- May, A.P., Misura, K.M., Whiteheart, S.W. and Weis, W.I. 1999. Crystal structure of the amino-terminal domain of *N*-ethylmaleimide-sensitive fusion protein. *Nat. Cell. Biol.* **1**: 175-182.
- Mazzarello, P., Garbarino, C. and Calligaro, A. 2009. How Camillo Golgi became "the Golgi". *FEBS Lett.* **583**: 3732-3737.
- McDonald, P.H., Cote, N.L., Lin, F.T., Premont, R.T., Pitcher, J.A. and Lefkowitz, R.J. 1999. Identification of NSF as a β -arrestin1-binding protein. Implications for β_2 -adrenergic receptor regulation. *J. Biol. Chem.* **274**: 10677-10680.
- McFadden, G.I. and Melkonian, M. 1986. Golgi apparatus activity and membrane flow during scale biogenesis in the green flagellate *Scherffelia dubia* (*Prasinophyceae*). I: Flagellar regeneration. *Protoplasma* **130**: 186-198.
- Mogelsvang, S., Gomez-Ospina, N., Soderholm, J., Glick, B.S. and Staehelin, L.A. 2003. Tomographic evidence for continuous turnover of Golgi cisternae in *Pichia pastoris*. *Mol. Biol Cell* **14**: 2277-2291.
- Mollenhauer, H.H. and Morré, D.J. 1991. Perspectives on Golgi apparatus form and function. *J. Electron Microsc. Tech.* **17**: 2-14.
- Nakano, A. 2004. Yeast Golgi apparatus--dynamics and sorting. *Cell Mol. Life Sci.* **61**: 186-191.
- Nakano, A. 2015. Cell biology: Polarized transport in the Golgi apparatus. *Nature* **521**:

427-428.

Nakano, A. and Muramatsu, M. 1989. A novel GTP-binding protein, Sar1p, is involved in transport from the endoplasmic reticulum to the Golgi apparatus. *J. Cell Biol.* **109**: 2677-2691.

Nakano, R.T., Matsushima, R., Nagano, A.J., Fukao, Y., Fujiwara, M., Kondo, M., Nishimura, M. and Hara-Nishimura, I. 2012. ERMO3/MVP1/GOLD36 is involved in a cell type-specific mechanism for maintaining ER morphology in *Arabidopsis thaliana*. *PLoS One* **7**: e49103.

Nakano, R.T., Matsushima, R., Ueda, H., Tamura, K., Shimada, T., Li, L., Hayashi, Y., Kondo, M., Nishimura, M. and Hara-Nishimura, I. 2009. GNOM-LIKE1/ERMO1 and SEC24a/ERMO2 are required for maintenance of endoplasmic reticulum morphology in *Arabidopsis thaliana*. *Plant Cell* **21**: 3672-3685.

Naramoto, S., Otegui, M.S., Kutsuna, N., de Rycke, R., Dainobu, T., Karampelias, M., Fujimoto, M., Feraru, E., Miki, D., Fukuda, H., Nakano, A. and Friml, J. 2014. Insights into the localization and function of the membrane trafficking regulator GNOM ARF-GEF at the Golgi apparatus in *Arabidopsis*. *Plant Cell* **26**: 3062-3076.

Nebenführ, A., Gallagher, L.A., Dunahay, T.G., Frohlick, J.A., Mazurkiewicz, A.M., Meehl, J.B. and Staehelin, L.A. 1999. Stop-and-go movements of plant Golgi stacks are mediated by the acto-myosin system. *Plant Physiol.* **121**: 1127-1142.

Neuwald, A.F. 1999. The hexamerization domain of N-ethylmaleimide-sensitive factor: structural clues to chaperone function. *Structure* **7**: R19-23.

Neuwald, A.F., Aravind, L., Spouge, J.L. and Koonin, E.V. 1999. AAA+: A class of chaperone-like ATPases associated with the assembly, operation, and disassembly of protein complexes. *Genome Res.* **9**: 27-43.

Nilsson, T., Au, C.E. and Bergeron, J.J. 2009. Sorting out glycosylation enzymes in the

Golgi apparatus. *FEBS Lett.* **583**: 3764-3769.

Ogura, T., Whiteheart, S.W. and Wilkinson, A.J. 2004. Conserved arginine residues implicated in ATP hydrolysis, nucleotide-sensing, and inter-subunit interactions in AAA and AAA+ ATPases. *J. Struct. Biol.* **146**: 106-112.

Orci, L., Ravazzola, M., Volchuk, A., Engel, T., Gmachl, M., Amherdt, M., Perrelet, A., Sollner, T.H. and Rothman, J.E. 2000. Anterograde flow of cargo across the golgi stack potentially mediated via bidirectional "percolating" COPI vesicles. *Proc. Natl. Acad. Sci. U. S. A.* **97**: 10400-10405.

Orci, L., Starnes, M., Ravazzola, M., Amherdt, M., Perrelet, A., Söllner, T.H. and Rothman, J.E. 1997. Bidirectional transport by distinct populations of COPI-coated vesicles. *Cell* **90**: 335-349.

Orso, G., Penden, D., Liu, S., Tosetto, J., Moss, T.J., Faust, J.E., Micaroni, M., Egorova, A., Martinuzzi, A., McNew, J.A. and Daga, A. 2009. Homotypic fusion of ER membranes requires the dynamin-like GTPase atlastin. *Nature* **460**: 978-983.

Owen, D.J. and Schiavo, G. 1999. A handle on NSF. *Nat. Cell Biol.* **1**: E127-128.

Otsu, N. 1979. A threshold selection method from gray-level histograms. *IEEE Trans. Sys., Man., Cyber.* **9**: 62-66.

Pallanck, L., Ordway, R.W., Ramaswami, M., Chi, W.Y., Krishnan, K.S. and Ganetzky, B. 1995. Distinct roles for *N*-ethylmaleimide-sensitive fusion protein (NSF) suggested by the identification of a second *Drosophila* NSF homolog. *J. Biol. Chem.* **270**: 18742-18744.

Papanikou, E., Day, K.J., Austin, J. and Glick, B.S. 2015. COPI selectively drives maturation of the early Golgi. *ELife* **4**: e13232.

Papanikou, E. and Glick, B.S. 2014. Golgi compartmentation and identity. *Curr. Opin.*

Cell Biol. **29**: 74-81.

Park, S.Y., Yang, J.S., Schmider, A.B., Soberman, R.J. and Hsu, V.W. 2015. Coordinated regulation of bidirectional COPI transport at the Golgi by CDC42. *Nature* **521**: 529-352.

Pelham, H.R. 1998. Getting through the Golgi complex. *Trends Cell Biol.* **8**: 45-49.

Pelham, H.R. and Rothman, J.E. 2000. The debate about transport in the Golgi--two sides of the same coin? *Cell* **102**: 713-719.

Pimpl, P., Movafeghi, A., Coughlan, S., Denecke, J., Hillmer, S. and Robinson, D.G. 2000. In situ localization and in vitro induction of plant COPI-coated vesicles. *Plant Cell* **12**: 2219-2236.

Preuss, D., Mulholland, J., Franzusoff, A., Segev, N. and Botstein, D. 1992. Characterization of the *Saccharomyces* Golgi complex through the cell cycle by immunoelectron microscopy. *Mol. Biol. Cell* **3**: 789-803.

Rabouille, C. and Klumperman, J. 2005. Opinion: The maturing role of COPI vesicles in intra-Golgi transport. *Nat. Rev. Mol. Cell Biol.* **6**: 812-817.

Rabouille, C., Levine, T.P., Peters, J.M. and Warren, G. 1995. An NSF-like ATPase, p97, and NSF mediate cisternal regrowth from mitotic Golgi fragments. *Cell* **82**: 905-914.

Rambourg, A., Clermont, Y., Ovtracht, L. and Képès, F. 1995. Three-dimensional structure of tubular networks, presumably Golgi in nature, in various yeast strains: a comparative study. *Anat. Rec.* **243**: 283-293.

Richter, S., Anders, N., Wolters, H., Beckmann, H., Thomann, A., Heinrich, R., Schrader, J., Singh, M.K., Geldner, N., Mayer, U. and Jürgens, G. 2010. Role of the *GNOM* gene in *Arabidopsis* apical-basal patterning--From mutant phenotype to cellular

mechanism of protein action. *Eur. J. Cell Biol.* **89**: 138-144.

Rice, L.M. and Brunger, A.T. 1999. Crystal structure of the vesicular transport protein Sec17: implications for SNAP function in SNARE complex disassembly. *Mol. Cell* **4**: 85-95.

Richter, S., Geldner, N., Schrader, J., Wolters, H., Stierhof, Y.D., Rios, G., Koncz, C., Robinson, D.G. and Jürgens, G. 2007. Functional diversification of closely related ARF-GEFs in protein secretion and recycling. *Nature* **448**: 488-492.

Ritzenthaler, C., Nebenführ, A., Movafeghi, A., Stussi-Garaud, C., Behnia, L., Pimpl, P., Staehelin, L.A. and Robinson, D.G. 2002. Reevaluation of the effects of brefeldin A on plant cells using tobacco Bright Yellow 2 cells expressing Golgi-targeted green fluorescent protein and COPI antisera. *Plant Cell* **14**: 237-261.

Robinson, D.G., Brandizzi, F., Hawes, C. and Nakano, A. 2015. Vesicles versus Tubes: Is Endoplasmic Reticulum-Golgi Transport in Plants Fundamentally Different from Other Eukaryotes? *Plant Physiol.* **168**: 393-406.

Rothman, J.E. and Wieland, F.T. 1996. Protein sorting by transport vesicles. *Science* **272**: 227-234.

Ryu, J.K., Jahn, R. and Yoon, T.Y. 2016. Review: Progresses in understanding N-ethylmaleimide sensitive factor (NSF) mediated disassembly of SNARE complexes. *Biopolymers* **105**: 518-531.

Saito, C. and Ueda, T. 2009. Chapter 4: functions of RAB and SNARE proteins in plant life. *Int. Rev. Cell Mol. Biol.* 2009. **274**: 183-233.

Sanderfoot, A. 2007. Increases in the number of SNARE genes parallels the rise of multicellularity among the green plants. *Plant Physiol.* **144**: 6-17.

Sanderfoot, A.A., Assaad, F.F. and Raikhel, N.V. 2000. The Arabidopsis genome. An

abundance of soluble *N*-ethylmaleimide-sensitive factor adaptor protein receptors. *Plant Physiol.* **124**: 1558-1569.

Sanyal, S. and Krishnan, K.S. 2001. Lethal comatose mutation in *Drosophila* reveals possible role for NSF in neurogenesis. *Neuroreport* **12**: 1363-1366.

Sato, K. and Nakano, A. 2005. Dissection of COPII subunit-cargo assembly and disassembly kinetics during Sar1p-GTP hydrolysis. *Nat. Struct. Mol. Biol.* **12**: 167-174.

Sato, K. and Nakano, A. 2007. Mechanisms of COPII vesicle formation and protein sorting. *FEBS Lett.* **581**: 2076-2082.

Scales, S.J., Yoo, B. Y. and Scheller, R.H. 2001. The ionic layer is required for efficient dissociation of the SNARE complex by α -SNAP and NSF. *Proc. Natl. Acad. Sci. U. S. A.* **98**: 14262-14267.

Schneeberger, K. and Weigel, D. 2011. Fast-forward genetics enabled by new sequencing technologies. *Trends Plant Sci.* **16**: 282-288.

Sengupta, D. and Linstedt, A.D. 2011. Control of organelle size: the Golgi complex. *Annu. Rev. Cell Dev. Biol.* **27**: 57-77.

Serafini, T., Stenbeck, G., Brecht, A., Lottspeich, F., Orci, L., Rothman, J.E. and Wieland, F.T. 1991. A coat subunit of Golgi-derived non-clathrin-coated vesicles with homology to the clathrin-coated vesicle coat protein β -adaptin. *Nature* **349**: 215-220.

Söllner, T., Bennett, M.K., Whiteheart, S.W., Scheller, R.H. and Rothman, J.E. 1993. A protein assembly-disassembly pathway in vitro that may correspond to sequential steps of synaptic vesicle docking, activation, and fusion. *Cell* **75**: 409-418.

Sparkes, I. and Brandizzi, F. 2012. Fluorescent protein-based technologies: shedding new light on the plant endomembrane system. *Plant J.* **70**: 96-107.

Staehelein, L.A. and Kang, B.H. 2008. Nanoscale architecture of endoplasmic reticulum export sites and of Golgi membranes as determined by electron tomography. *Plant Physiol.* **147**: 1454-1468.

Steel, G.J., Harley, C., Boyd, A. and Morgan, A. 2000. A screen for dominant negative mutants of *SEC18* reveals a role for the AAA protein consensus sequence in ATP hydrolysis. *Mol. Biol. Cell* **11**: 1345-1356.

Storrie, B., Micaroni, M., Morgan, G.P., Jones, N., Kamykowski, J.A., Wilkins, N., Pan, T.H. and Marsh, B.J. 2012. Electron tomography reveals Rab6 is essential to the trafficking of *trans*-Golgi clathrin and COPI-coated vesicles and the maintenance of Golgi cisternal number. *Traffic* **13**: 727-744.

Suda, Y., Kurokawa, K. and Nakano, A. 2018. Regulation of ER-Golgi transport dynamics by GTPases in budding yeast. *Front. Cell Dev. Biol.* **5**: 122.

Südhof, T.C. 2013. Neurotransmitter release: the last millisecond in the life of a synaptic vesicle. *Neuron* **80**: 675-690.

Sutton, R.B., Fasshauer, D., Jahn, R. and Brunger, A.T. 1998. Crystal structure of a SNARE complex involved in synaptic exocytosis at 2.4 Å resolution. *Nature* **395**: 347-353.

Szul, T. and Sztul, E. 2011. COPII and COPI traffic at the ER-Golgi interface. *Physiology (Bethesda)* **26**: 348-364.

Tachikawa, M. and Mochizuki, A. 2017. Golgi apparatus self-organizes into the characteristic shape via postmitotic reassembly dynamics. *Proc. Natl. Acad. Sci. U. S. A.* **114**: 5177-5182.

Takei, K. and Haucke, V. 2001. Clathrin-mediated endocytosis: membrane factors pull the trigger. *Trends Cell Biol.* **11**: 385-391.

Takeuchi, M., Ueda, T., Sato, K., Abe, H., Nagata, T. and Nakano, A. 2000. A dominant negative mutant of Sar1 GTPase inhibits protein transport from the endoplasmic reticulum to the Golgi apparatus in tobacco and *Arabidopsis* cultured cells. *Plant J.* **23**: 517-525.

Takeuchi, M., Ueda, T., Yahara, N. and Nakano, A. 2002. Arf1 GTPase plays roles in the protein traffic between the endoplasmic reticulum and the Golgi apparatus in tobacco and *Arabidopsis* cultured cells. *Plant J.* **31**: 499-515.

Tang, B.L., Wang, Y., Ong, Y.S. and Hong, W. 2005. COPII and exit from the endoplasmic reticulum. *Biochim. Biophys. Acta.* **1744**: 293-303.

Teh, O.K. and Moore, I. 2007. An ARF-GEF acting at the Golgi and in selective endocytosis in polarized plant cells. *Nature* **448**: 493-496.

Uemura, T., Ueda, T., Ohniwa, R.L., Nakano, A., Takeyasu, K. and Sato, M.H. 2004. Systematic analysis of SNARE molecules in *Arabidopsis*: dissection of the post-Golgi network in plant cells. *Cell Struct. Funct.* **29**: 49-65.

Uchida, N., Sakamoto, T., Kurata, T. and Tasaka, M. 2011. Identification of EMS-induced causal mutations in a non-reference *Arabidopsis thaliana* accession by whole genome sequencing. *Plant Cell Physiol.* **52**: 716-722.

Ueda, T. and Nakano, A. 2002. Vesicular traffic: an integral part of plant life. *Curr. Opin. Plant Biol.* **5**: 513-517.

Weber, T., Zemelman, B.V., McNew, J.A., Westermann, B., Gmachl, M., Parlati, F., Söllner, T.H. and Rothman, J.E. 1998. SNAREpins: minimal machinery for membrane fusion. *Cell* **92**: 759-772.

Waters, M.G., Serafini, T. and Rothman, J.E. 1991. 'Coatomer': a cytosolic protein complex containing subunits of non-clathrin-coated Golgi transport vesicles. *Nature* **349**: 248-251.

Weidman, P.J., Melançon, P., Block, M.R. and Rothman, J.E. 1989. Binding of an *N*-ethylmaleimide-sensitive fusion protein to Golgi membranes requires both a soluble protein(s) and an integral membrane receptor. *J. Cell Biol.* **108**: 1589-1596.

Whiteheart, S.W., Rossnagel, K., Buhrow, S.A., Brunner, M., Jaenicke, R. and Rothman, J.E. 1994. *N*-ethylmaleimide-sensitive fusion protein: a trimeric ATPase whose hydrolysis of ATP is required for membrane fusion. *J. Cell Biol.* **126**: 945-954.

Whiteheart, S.W., Schraw, T. and Matveeva, E.A. 2001. *N*-ethylmaleimide sensitive factor (NSF) structure and function. *Int. Rev. Cytol.* **207**: 71-112.

Xu, J. and Scheres, B. 2005. Dissection of Arabidopsis ADP-RIBOSYLATION FACTOR 1 function in epidermal cell polarity. *Plant Cell* **17**: 525-536.

Yang, J.S., Valente, C., Polishchuk, R.S., Turacchio, G., Layre, E., Moody, D.B., Leslie, C.C., Gelb, M.H., Brown, W.J., Corda, D., Luini, A. and Hsu, V.W. 2011. COPI acts in both vesicular and tubular transport. *Nat. Cell Biol.* **13**: 996-1003.

Yu, R.C., Hanson, P.I., Jahn, R. and Brünger, A.T. 1998. Structure of the ATP-dependent oligomerization domain of *N*-ethylmaleimide sensitive factor complexed with ATP. *Nat. Struct. Biol.* **5**: 803-811.

Yu, R.C., Jahn, R. and Brunger, A.T. 1999. NSF N-terminal domain crystal structure: models of NSF function. *Mol. Cell* **4**: 97-107.

Zhang, M. and Hu, J. 2013. Homotypic fusion of endoplasmic reticulum membranes in plant cells. *Front. Plant Sci.* **4**: 514.

Zhao, C., Matveeva, E.A., Ren, Q. and Whiteheart, S.W. 2010. Dissecting the *N*-ethylmaleimide-sensitive factor: required elements of the N and D1 domains. *J. Biol. Chem.* **285**: 761-772.

Zhao, M. and Brunger, A.T. 2016. Recent Advances in Deciphering the Structure and Molecular Mechanism of the AAA+ ATPase *N*-Ethylmaleimide-Sensitive Factor (NSF). *J. Mol. Biol.* **428**: 1912-1926.

Zhao, M., Wu, S., Zhou, Q., Vivona, S., Cipriano, D.J., Cheng, Y. and Brunger, A.T. 2015. Mechanistic insights into the recycling machine of the SNARE complex. *Nature* **518**: 61-67.

Zheng, H., Kunst, L., Hawes, C. and Moore, I. 2004. A GFP-based assay reveals a role for RHD3 in transport between the endoplasmic reticulum and Golgi apparatus. *Plant J.* **37**: 398-414.

Zwiewka, M., Feraru, E., Möller, B., Hwang, I., Feraru, M.I., Kleine-Vehn, J., Weijers, D. and Friml, J. 2011. The AP-3 adaptor complex is required for vacuolar function in *Arabidopsis*. *Cell Res.* **21**: 1711-1722.